



2014-02-24

Inhibition of PIM and AXL Kinases As Potential Treatments for a Variety of Hematological Malignancies and Solid Tumors

Kent James Carpenter
Brigham Young University - Provo

Follow this and additional works at: <https://scholarsarchive.byu.edu/etd>

 Part of the [Cell and Developmental Biology Commons](#), and the [Physiology Commons](#)

BYU ScholarsArchive Citation

Carpenter, Kent James, "Inhibition of PIM and AXL Kinases As Potential Treatments for a Variety of Hematological Malignancies and Solid Tumors" (2014). *All Theses and Dissertations*. 3842.
<https://scholarsarchive.byu.edu/etd/3842>

This Thesis is brought to you for free and open access by BYU ScholarsArchive. It has been accepted for inclusion in All Theses and Dissertations by an authorized administrator of BYU ScholarsArchive. For more information, please contact scholarsarchive@byu.edu, ellen_amatangelo@byu.edu.

Inhibition of PIM and AXL Kinases as Potential Treatments for a Variety of Hematological
Malignancies and Solid Tumors

Kent J. Carpenter

A thesis submitted to the faculty of
Brigham Young University
in partial fulfillment of the requirements for the degree of
Master of Science

Marc D. Hansen, Chair
Juan A. Arroyo
Joshua L. Andersen

Department of Physiology and Developmental Biology
Brigham Young University

February 2014

Copyright © 2014 Kent J. Carpenter

All Rights Reserved

ABSTRACT

Inhibition of PIM and AXL Kinases as Potential Treatments for a Variety of Hematological Malignancies and Solid Tumors

Kent J. Carpenter

Department of Physiology and Developmental Biology, BYU

Master of Science

This thesis is divided into three chapters. In each case, the goal is to achieve inhibition of a growth kinase (PIM or AXL) and subsequent arrest of cell growth and induction of apoptosis (*in vitro* cell culture models) or decrease in tumor volume (*in vivo* xenograft studies).

Chapter one and chapter two discuss inhibition of proviral integration site for Moloney murine leukemia virus (PIM) kinases. The three PIM kinases, PIM-1, PIM-2, and PIM-3, are a subfamily of serine/threonine kinases that are known to be involved in signaling pathways as downstream effectors of signal transducer and activator of transcription-5 (STAT5) signaling and inhibitors of apoptosis. PIM kinases are implicated in a large percentage of hematological malignancies and solid tumors. Because they have been shown to correlate with disease progression and poor prognosis in many of these conditions, PIM kinase inhibitors are being developed and investigated for therapeutic use.

The aim of this study in chapter one was to evaluate the role of PIM 1, 2 and 3 in urothelial carcinomas, using second generation Pan-PIM kinase inhibitor TP-3654. Retrospective immunohistochemical analysis of bladder cancer specimens found that PIM 1, 2, and 3 was expressed in a significant number of cases. PIM-1 was expressed in 4 bladder cancer cell lines and TP-3654 treatment was able to inhibit BAD phosphorylation to induce apoptosis.

The second aim of this study was to investigate the effects of TP-3654 on the interaction of c-MYC with PIM kinase family members. The data indicate that PIM-1 only interacts with c-MYC in the acute myeloid leukemia (AML) and multiple myeloma (MM) cell lines studied, and that PIM-1 siRNA knockdown or treatment with TP-3654 is able to decrease this interaction.

The third chapter discusses inhibition of the receptor tyrosine kinase Axl. Pancreatic cancer is a highly lethal disease characterized by malignant cells that rapidly disseminate from the primary tumor to form local and distant metastases. Axl is overexpressed in over 50% of pancreatic cancers and expression of Axl in these cancers is highly associated with a poor prognostic outcome for patients. Small molecule inhibitors of AXL are currently under investigation, as AXL is associated with cell migration mediated by epithelial-mesenchymal transition (EMT). The aim of this study was to investigate the effects of a small molecule inhibitor of AXL, TP-0903, on pancreatic cancer cell lines. Consistent with the known function of Axl, TP-0903 inhibited Gas6-induced migration and invasion of pancreatic cancer cells *in vitro* and potently induced apoptosis. Additionally, we found that inhibition of AXL decreased expression of EMT marker genes and induced mesenchymal pancreatic cancer cell lines to take on an epithelial phenotype. TP-0903 also significantly inhibited the growth of pancreatic cancer cell lines grown in xenograft tumor mouse model and taken together, the results suggest Axl is a potential therapeutic target in pancreatic cancer and TP-0903 as a potential therapeutic agent.

Keywords: STAT5 signaling, Bcl-2, BAD, apoptosis, carcinoma, oncogene, migration, metastasis, EMT, xenograft

ACKNOWLEDGMENTS

I would first like to thank Dr. David Bearss, my former committee chair who has since left Brigham Young University, for the remarkable opportunity to work with him on these projects. Dr. Bearss has been an outstanding mentor from the first day I met him, and has always pushed me to succeed, with my interests and goals as a priority.

I am also especially grateful to our former lab manager, Lee Call, for his time and efforts in teaching me virtually all the lab techniques I employed in my projects. Dr. Steve Warner and Dr. Bret Stephens of Tolero Pharmaceuticals (who work with Dr. Bearss) have also been helpful in preparing our manuscripts, especially the *in vivo* data, for submission.

I would also like to thank the other members of my graduate committee. First, I appreciate Dr. Marc Hansen's expertise and help with the migration assays contained in the AXL portion of this manuscript. Additionally, I'm grateful for all of the support he has provided, from the beginning of my graduate studies until now, as he has agreed to become my committee chair in Dr. Bearss's absence.

Secondly, I'm grateful to Dr. Juan Arroyo for agreeing to become one of my graduate committee members on short notice.

Finally, I'm grateful to Dr. Josh Andersen who has been supportive of all of my projects from the beginning.

TABLE OF CONTENTS

TITLE PAGE.....	i
ABSTRACT.....	ii
ACKNOWLEDGMENTS.....	iii
TABLE OF CONTENTS.....	iv
LIST OF TABLES.....	viii
LIST OF FIGURES.....	ix
CHAPTER 1: A Small Molecule Inhibitor of PIM kinases As a Potential Treatment For Urothelial Carcinomas.....	1
Abstract.....	1
Introduction.....	2
Materials and Methods.....	4
Synthesis of TP-3654.....	4
PIM Kinase IC ₅₀ and K _i Determinations.....	4
Cell Lines.....	5
hERG Assay.....	5
Statistical Analysis and IC ₅₀ /EC ₅₀ Determination.....	6
shRNA Transduction.....	6
RT-PCR.....	6
Colony Formation Assay.....	7
Cell Lysis and Western Blots.....	7
Apoptosis Assays.....	8
PIM-1 siRNA.....	8
TP-3654 Treatment.....	9
Urothelial Carcinoma Pathology Cases.....	9

Tumor Xenograft Studies.....	9
Pharmacokinetic Study.....	10
Results.....	11
Discussion.....	13
CHAPTER 2: Inhibition of PIM kinases Results in Downregulation of Oncogenic CMYC Signaling and Induction of Apoptosis in Hematological Malignancies, Including Acute Myeloid Leukemia and Multiple Myeloma.....	17
Abstract.....	17
Introduction.....	18
Materials and Methods.....	20
Synthesis of TP-3654.....	20
Cell Lines.....	20
Cell Lysis and Western Blots.....	21
Apoptosis Assays.....	21
PIM-1 siRNA.....	22
TP-3654 Immunoprecipitation Treatment.....	22
Immunoprecipitation.....	22
Results.....	23
Discussion.....	23
CHAPTER 3: Inhibition of The Tyrosine Kinase Receptor AXL Blocks Cell Invasion and Promotes Apoptosis in Pancreatic Cancer Cells.....	25
Abstract.....	25
Introduction.....	26
Materials and Methods.....	29
Biochemical Assays.....	29

pAKT ELISA.....	29
Migration Assays.....	29
Apoptosis Assays.....	29
Real Time PCR.....	30
Western Blots.....	30
Soluble AXL Data.....	31
Xenograft Study.....	31
Pharmacokinetic Data.....	31
Results.....	32
TP-0903 is a Multi-Targeted Kinase Inhibitor With Potent Activity Against AXL.....	32
Migration Assays.....	32
TP-0903 Potently Induces Apoptosis in Pancreatic Cancer Cell Lines.....	32
AXL Inhibition by TP-0903 Significantly Reduces Expression of EMT Marker Genes.....	32
sAXL in Pancreatic Cancer.....	33
TP-0903 Reduces Tumor Volume in Pancreatic Cancer Xenografts.....	34
Discussion.....	34
REFERENCES.....	38
FIGURE LEGENDS.....	48
TABLES.....	54
Table 1.1: Biochemical, FLT3, and hERG potency comparison of TP-3654 and SGI-1776.....	54
Table 1.2: PIM kinase expression in urothelial carcinoma.....	54
FIGURES.....	55
Figure 1.1: Structure and Analysis of TP-3654.....	55

Figure 1.2: Validation of PIM-1 in solid tumor models <i>in vitro</i>	56
Figure 1.3: TP-3654 induces apoptosis and inhibits BAD phosphorylation in bladder Cancer cell lines.....	57
Figure 1.4: PIM-2 kinase expression in Urothelial Carcinoma Cases.....	58
Figure 1.5: TP-3654 inhibits the growth of established solid tumor xenografts.....	59
Figure 1.6: Oral PK data for TP-3654.....	60
Figure 2.1: PIM-1 alone interacts with cMYC in AML and MM Cell Lines.....	61
Figure 2.2: PIM-1 siRNA or TP-3654 decreases the PIM-1-cMYC interaction in AML and MM Cell Lines.....	62
Figure 2.3: TP-3654 Induces Apoptosis in AML and MM Cell Lines.....	63
Figure 3.1: TP-0903 is a potent AXL kinase inhibitor.....	64
Figure 3.2: TP-0903 reduces pAKT levels upon GAS6 stimulation independent of sAXL levels.....	65
Figure 3.3: Cell migration is reduced with AXL inhibitor TP-0903.....	66
Figure 3.4: TP-0903 effectively induces apoptosis in both the PANC-1 and PSN-1 cell lines within 24 hours at concentrations as low as 0.1µM.....	67
Figure 3.5: TP-0903 effectively suppresses expression of EMT marker genes in pancreatic cancer cell lines.....	68
Figure 3.6: Soluble AXL is a potential marker for metastatic cancer progression.....	69
Figure 3.7: TP-0903 reduces tumor volume in PSN-1 xenograft studies and displays favorable oral pharmacokinetics.....	70
CURRICULUM VITAE.....	71

LIST OF TABLES

Table 1.1: Biochemical, FLT3, and hERG potency comparison of TP-3654
and SGI-1776.....54

Table 1.2: PIM kinase expression in urothelial carcinoma.....54

LIST OF FIGURES

Figure 1.1: Structure and Analysis of TP-3654.....	55
Figure 1.2: Validation of PIM-1 in solid tumor models <i>in vitro</i>	56
Figure 1.3: TP-3654 induces apoptosis and inhibits BAD phosphorylation in bladder Cancer cell lines.....	57
Figure 1.4: PIM-2 kinase expression in Urothelial Carcinoma Cases.....	58
Figure 1.5: TP-3654 inhibits the growth of established solid tumor xenografts.....	59
Figure 1.6: Oral PK data for TP-3654.....	60
Figure 2.1: PIM-1 alone interacts with cMYC in AML and MM Cell Lines.....	61
Figure 2.2: PIM-1 siRNA or TP-3654 decreases the PIM-1-cMYC interaction in AML and MM Cell Lines.....	62
Figure 2.3: TP-3654 Induces Apoptosis in AML and MM Cell Lines.....	63
Figure 3.1: TP-0903 is a potent AXL kinase inhibitor.....	64
Figure 3.2: TP-0903 reduces pAKT levels upon GAS6 stimulation independent of sAXL levels.....	65
Figure 3.3: Cell migration is reduced with AXL inhibitor TP-0903.....	66
Figure 3.4: TP-0903 effectively induces apoptosis in both the PANC-1 and PSN-1 cell lines within 24 hours at concentrations as low as 0.1µM.....	67
Figure 3.5: TP-0903 effectively suppresses expression of EMT marker genes in pancreatic cancer cell lines.....	68
Figure 3.6: Soluble AXL is a potential marker for metastatic cancer progression.	69
Figure 3.7: TP-0903 reduces tumor volume in PSN-1 xenograft studies and displays favorable oral pharmacokinetics.....	70

CHAPTER 1: A Small Molecule Inhibitor of PIM Kinases As a Potential Treatment for Urothelial Carcinomas

Kent J. Carpenter¹, Jason M. Foulks², Bai Luo³, Yong Xu³, Anna Senina³, Rebecca Nix³, Ashley Chan³, Adrienne Clifford³, Marcus Wilkes³, David Vollmer³, Benjamin Brenning³, Shannon Merx³, Shuping Lai³, Michael V. McCullar³, Koc-Kan Ho³, Daniel J. Albertson⁴, Lee T. Call⁵, Jared J. Bearss⁶, Sheryl Tripp⁷, Ting Liu⁴, Bret J. Stephens⁵, Alexis Mollard⁵, Steven L. Warner⁵, Steven B. Kanner³, and David J. Bearss⁵

Authors Affiliation: 1. Department of Physiology and Developmental Biology, BYU, Provo, UT. 2. AlloCure Inc., Salt Lake City, UT. 3. Astex Pharmaceuticals Inc., Salt Lake City, UT. 4. Department of Pathology, University of Utah School of Medicine, Salt Lake City, UT. 5. Tolero Pharmaceuticals, Inc., Lehi, UT. 6. Huntsman Cancer Institute, University of Utah, Salt Lake City, UT. 7. R&D, ARUP Laboratories, Salt Lake City, UT.

Abstract

The proto-oncogene PIM kinases (PIM-1, PIM-2, PIM-3) are serine/threonine kinases that are involved in a number of signaling pathways important to cancer cells. PIM kinases act in downstream effector functions as inhibitors of apoptosis and as positive regulators of G1-S phase progression through the cell cycle. PIM kinases are upregulated in multiple cancer indications, including lymphoma, leukemia, multiple myeloma, prostate, gastric, and head & neck cancers. Overexpression of one or more PIM family members in patient tumors frequently correlates with poor prognosis. The aim of this investigation was to evaluate PIM expression in low- and high-grade urothelial carcinoma, and to assess for expression that may contribute to disease progression and serve as a potential site for targeted therapy. One hundred and thirty seven cases of urothelial carcinoma were included in this retrospective study of surgical biopsy and resection specimens from the University of Utah Department of Pathology (retrieved from 2008-2011). Our second generation PIM inhibitor, TP-3654, displays sub- μ M activity in pharmacodynamic marker modulation, proliferation and 2D colony formation assays using the UM-UC-3 bladder cancer cell line. TP-3654 was also found to induce apoptosis in the T24, RT4, and UM-UC-3 bladder cancer cell lines. TP-3654 displays favorable hERG and CYP inhibition profiles

compared with the first generation PIM inhibitor, SGI-1776, and has demonstrated excellent oral bioavailability. *In vivo* xenograft studies using a bladder cancer cell line model show that PIM kinase inhibition can reduce the growth of this tumor model suggesting that PIM kinase inhibitors may be active in human urothelial carcinomas.

Introduction

The serine/threonine family of PIM kinases were first identified as proto-oncogenes activated in T-cell lymphomas induced by murine leukemia viruses. The PIM kinase family comprises three members (PIM-1, PIM-2, and PIM-3) with six different isoforms from alternate translation initiating sites (1-5). Although the PIM kinase family is transcriptionally and translationally regulated in cells, these kinases lack a regulatory domain and are constitutively activated when expressed (6-10).

Expression of PIM-1 is induced by several cytokines, which often activate STAT5 in conjunction with PIM-1. In fact, the Pim kinases are target genes of STAT3 and STAT5 signaling and are correlated with levels of STAT signaling (11-15). They often form complexes with Hsp70 and Hsp90 for stabilization, but are eventually polyubiquitinated for proteasomal degradation (11-15).

Although they were first implicated in human acute myeloid leukemia (AML) cases, PIM kinases are over-expressed in many different types of malignancies including hematologic and solid tumors. Specifically, over-expression has been identified in bladder, prostate, head & neck, and several hematologic cancers. Over-expression of PIM kinases is often associated with poor prognosis in each of these cancers. The PIM kinases have a variety of downstream targets that are thought to contribute to tumor growth. In particular, PIM kinases target the pro-apoptotic Bcl2-associated death promoter (BAD) family members and inhibit apoptosis (6-10).

In addition, it has been shown in prostate tumors that PIM-1 and c-MYC associate together, resulting in transcriptional upregulation and stabilization of c-MYC. Such prostate tumors exhibited higher Gleason scores and differentiation (16-20). Functionally, expression of PIM kinases in tumors correlates with increased cell survival and reduced apoptosis, implicating the family members as attractive targets for disruptive therapy.

Crystal structures for both PIM-1 and PIM-2 have been used to understand their unique ATP binding pocket and for computational and medicinal chemistry efforts to develop inhibitors. The hinge region of PIM kinases is unusual in that it contains a proline not generally present in serine/threonine kinase hinges, as well as other unique residues in the ATP binding cleft (21-26). Astex Pharmaceuticals, Inc. (formerly SuperGen, Inc.) developed an imidazopyridazine based inhibitor, SGI-1776, that exhibited potent anti-PIM activity both *in vitro* and *in vivo* in a variety of preclinical models (27-30). Studies have demonstrated that SGI-1776 exhibited potent anti-tumor activity in preclinical models of FLT3-ITD mutant AML (30-32). Investigators have demonstrated that the observed activity in this model system may be due to the predominant anti-FLT3 activity (33). In contrast, models without the FLT3-ITD mutation were sensitive to SGI-1776, suggesting PIM-specific activity may be responsible for the observed anti-proliferative effects (34-39). Ultimately, SGI-1776 was evaluated in a phase I clinical trial recruiting patients with either prostate cancer or non-Hodgkin's lymphoma. However, the trial was terminated early due to a narrow therapeutic window, likely attributed to inhibition of the cardiac potassium channel hERG (human Ether-à-go-go-Related Gene) also observed with SGI-1776 in functional assays.

Our recent efforts focused on identifying a novel PIM kinase inhibitor with a unique anti-kinase profile and attractive pharmaceutical properties. In this report, we describe the discovery

and characterization of a second-generation small-molecule PIM kinase inhibitor, TP-3654 (SGI 9481), which exhibits potent activity against all three PIM kinases, but with reduced activity against FLT3. Further, oral administration of TP-3654 led to reduced tumor growth of established human bladder carcinoma xenografts at safe and tolerated doses.

PIM-1, 2, and 3 expression has been well characterized in several leukemic and prostate cancers. In addition, it has been shown that PIM-1 was observed in invasive and non-invasive urothelial carcinoma specimens, with a higher incidence in invasive cancer (40). Because PIM kinases' role in bladder cancer is less well characterized, we sought to further evaluate PIM expression in low- and high-grade urothelial carcinoma. Seventy-two cases of urothelial carcinoma were included in this retrospective study of surgical biopsy and resection specimens from the University of Utah Department of Pathology. We further sought to evaluate the activity of TP-3654 in bladder cancer cell lines and xenograft models. Overall, the data presented here provide preclinical activity to support the potential application of this inhibitor in urothelial carcinomas.

Materials and Methods

Synthesis of TP-3654

TP-3654 (4-((3-(3-(Trifluoromethyl)phenyl)imidazo[1,2-b]pyridazin-6-yl)amino) -*trans*-cyclohexyl)propan-2-ol) was prepared according to United States Patent Application Publication US2012/0058997 (Imidazo[1,2-B]pyridazine and pyrazolo[1,5-A]pyrimidine derivatives and their use as protein kinase inhibitors).

PIM Kinase IC₅₀ and K_i Determinations

PIM kinase K_i determinations, TP-3654 selectivity screens and IC₅₀ determinations were

performed by Reaction Biology (Malvern, PA). For K_i determination, PIM-1, PIM-2 or PIM-3 were incubated with 10-dose, 3-fold serial dilutions of TP-3654 starting with 10 μ M using five different concentrations of ATP (25, 50, 100, 250 and 500 μ M ATP for PIM-1; 5, 10, 20, 50 and 100 μ M ATP for PIM-2 and PIM-3), and the activity was measured at 0, 5, 10, 15, 20, 30, 45, 60, 75, 90, 105 and 120 minutes. The data was analyzed in a Michaelis–Menten plot to determine apparent K_m and K_i values using GraFit software using a mixed inhibition equation for global fit. For selectivity, 1 μ M TP-3654 was tested against 336 kinases at a concentration of 10 μ M ATP. IC_{50} determinations of PI3K (α , β , δ , and γ) and all kinases inhibited >50% from the initial screen were performed using 10-dose, 3-fold serial dilutions of TP-3654 starting with 10 μ M at K_m ATP concentrations for each kinase.

Cell Lines

The T24, RT4, J82, and UM-UC3 bladder cancer cell lines were obtained directly from the American Type Culture Collection (ATCC) in Manassas, VA, USA. These cell lines were passaged for less than 6 months before use in the described assays and were authenticated by ATCC. The MV4-11 and other cell lines used were not authenticated by the authors.

hERG Assay

TP-3654 was tested for effect on hERG potassium channels by automated patch clamp method (QPatch^{HTX}) at WuXi AppTec (Shanghai, China). Chinese hamster ovary cells stably expressing hERG potassium channels from Aviva Biosciences were tested with TP-3654 at six concentrations, 3-fold dilution starting at 30 μ M with a final DMSO concentration of 0.15%, and compared to vehicle (negative) control and Amitriptyline (positive) controls. Percent of control (vehicle) values were calculated in duplicate for each concentration of drug, and curve-fitting and IC_{50} calculations were performed by QPatch Assay Software.

Statistical Analysis and IC₅₀/EC₅₀ Determination

Statistical analyses were performed by parametric ANOVA test. IC₅₀ and EC₅₀ values were determined using GraphPad Prism software (La Jolla, CA).

shRNA Transduction

UM-UC-3 cells (2.5×10^5) were seeded in a 6-well plate in complete RPMI 1640 media, and allowed to adhere overnight at 37°C in 5% CO₂. Cells were transduced with 8 µg/mL polybrene (Sigma-Aldrich) and Lentiviral particles at an MOI of 50 based on titer values pre-determined by Sigma-Aldrich using a p24 ELISA for each batch of shRNA. Following overnight transduction, viral particle containing media was removed and replaced with fresh complete media, and cells were cultured for an additional 48h at 37°C in 5% CO₂. Cells were trypsinized and fractions of the transduced cells were collected for colony formation growth assays, while the remaining cells were collected for RNA and protein isolation.

RT-PCR

RNA from 0.5×10^6 cells was isolated on a QIAcube (Qiagen, Santa Clarita, CA) using the protocol for purification of total RNA from animal cells (QIAshredder homogenization and on-column DNase digest), and quantified using a Nanodrop 8000 spectrophotometer (Thermo Electron, West Palm Beach, FL). Total RNA (1 µg) was converted to cDNA in a 20 µl reaction using the iScript cDNA synthesis kit (Bio-Rad, Hercules, CA) by incubating the reaction components for 5min at 25°C, 30min at 42°C, followed by 5min at 85°C. The cDNA reaction (2 µl) was used in a 20 µl PCR multiplex reaction using 1X FAM-labeled PIM-1, VIC-labeled actin Taqman primer sets and the Taqman gene expression master mix from Life Technologies on an iQ5 Real-Time PCR machine (Bio-Rad). An 8-point, half-log standard curve was generated for PIM-1 and actin messages using RNA from untreated cells. A linear trendline (with an R

squared value >0.99) was generated by plotting log concentrations of standard vs. Ct values generated from the real-time PCR reactions. Relative message levels from shRNA treated samples were calculated based on the standard curve, normalized to actin and compared to the non-target shRNA control.

Colony Formation Assay

For shRNA growth experiments, 500 UM-UC-3 cells were seeded in a 12-well plate 48 hours post-transduction and cultured for 8-10 days at 37°C in 5% CO₂. Cells were fixed with 4% paraformaldehyde in PBS, washed twice with PBS, and stained with a crystal violet solution (1% crystal violet, 10% ethanol in water). Stained cells were washed thrice with water, and imaged after drying on a GelCount colony counter (Oxford Optronix Ltd., Oxford, UK). Total staining intensity per well was determined by lysis of cells with 200 µl of Triton X-100 lysis buffer (1% Triton X-100, 50 mM Tris-HCl pH 7.4, 150 mM NaCl, 1 mM EDTA). Lysates (100 µl) from each well were transferred to a clear 96-well plate and absorbance at 560 nm was determined on an Envision microplate reader. IC₅₀ values were determined using GraphPad Prism software. For compound treated PC-3 and UM-UC-3, cells were seeded and stained as above, but were incubated with various concentrations of TP-3654 or DMSO one day after seeding.

Cell Lysis and Western Blots

In all applications, cells were washed with cold PBS and then treated with cell lysis solution (Cell Signaling). Lysates were centrifuged at 14,000g at 4°C according to the protocol. Protein levels were then measured and normalized using the BCA Protein Assay (Pierce). Normalized amounts of lysate were then run on pre-cast gels according to the manufacturer protocol, using MOPS running solution (Invitrogen). Gels were transferred using the iBlot system (Invitrogen) and then blocked for one hour in a 5% non-fat dry milk TBS-tween (TBST) solution. Blots were

treated with specified antibodies (all provided by Cell Signaling) diluted 1:1000 in 5% bovine serum albumin-TBST solution separately on a blot shaker overnight at 4°C. Blots were rinsed 3 times for 5 minutes each after antibody treatments, according to the protocol. The blots were treated with rabbit secondary antibody solutions (Cell Signaling) for 1 hour at room temperature diluted 1:1000 in a 5% non-fat dry milk TBST solution. As with the primary antibodies, the blots were rinsed 3 times for 5 minutes each before imaging with an ECL kit. The blots were stripped and then re-treated overnight with actin when used as a loading control. As explained previously, the blots were treated in antibody solution diluted 1:1000 in 5% BSA TBST solution overnight. Blots were treated with mouse secondary antibody (Pierce) and imaged as described previously.

Apoptosis Assays

Percentages of apoptotic bladder cancer (T24, RT4, UM-UC3) cells were measured using the violet radiometric membrane asymmetry probe/dead cell apoptosis kit for flow cytometry kit (Life Technologies). Cells were seeded in 6-well plates at a concentration of 2.5×10^5 cells per well, allowed to grow for 12 hours, and then drug treated with the specified concentrations of TP-3654 for 24 hours. Dyes were added and measured on the flow cytometer and gates were set according to the protocol from Invitrogen. Two independent experiments were carried out under identical conditions and then averaged to yield the given data. Treatment of UM-UC3 cells with cisplatin for 24 hours was used as a positive control.

PIM-1 siRNA

UM-UC3 bladder cancer cells were seeded in 6-well plates at a concentration 2.5×10^5 cells per well, allowed to grow for 12 hours, and then transfected with 75pmol of PIM-1 siRNA (QIAGEN), 75 pmol of prepared control siRNA (QIAGEN), or left untreated. Cells were

transfected using 6 μ L of Lipofectamine 2000 reagent (Invitrogen) diluted in Opti-MEM according to the protocol. Cells were treated with siRNA and transfection reagent for 24 hours before cell lysis, as described above. Levels of PIM-1 were analyzed by Western blot to confirm knockdown.

TP-3654 Treatment

UM-UC3 bladder cancer cells were seeded in 6-well plates at a concentration 2.5×10^5 cells per well, allowed to grow for 12 hours, and then treated with 3, 1, and 0.3 and 0.03 μ M of TP-3654 with 0.1% DMSO (vehicle) treated cells as a negative control. Cells were incubated with the drug for 12 hours and then lysed as described previously.

Urothelial Carcinoma Pathology Cases

One hundred and thirty seven cases of urothelial carcinoma were included in this retrospective study of surgical biopsy and resection specimens from the University of Utah Department of Pathology (retrieved from 2008-2011). Tissue was stained with commercially available antibodies against PIM-1, PIM-2, and PIM-3. Cases were classified into three groups according to WHO criteria (invasive high grade urothelial carcinoma (n=84), non-invasive high grade urothelial carcinoma/carcinoma in situ (n=32), and non-invasive low grade urothelial carcinoma (n=21)). Individual cases were reviewed by two of the authors (DA/TL) and given a score (0-4) based upon a percentage of cells demonstrating positive cytoplasmic and/or nuclear staining for each antibody (<5%=0; 5-25%=1; 26-50%=2; 51-75%=3; >75%=4). A score of 2 or greater was considered positive staining.

Tumor Xenograft Studies

Male and female Nu/Nu mice were purchased from Harlan Sprague Dawley (Indianapolis, IN). Female Nu/Nu mice were used for all xenograft evaluations with the exception of the PC-3

xenografts where male Nu/Nu mice were used. Cell lines were expanded *in vitro* in complete media, and if adherent were harvested by trypsin-EDTA, centrifuged and resuspended in PBS 1:1 with Matrigel (BD Biosciences). Cells were inoculated subcutaneously in the right hind flank of mice. When tumors reached 100-200 mm³ by caliper measurement, mice were randomized and dosing of TP-3654 or vehicle control began and continued every day for 5 days (QDx5) with 2 days off for 18-21 days. Tumor volumes and body weights were determined twice a week, and tumor weights were measured at the completion of the translational xenograft studies.

Pharmacokinetic Study

Female SD rats with jugular vein catheters were acquired from Charles River Laboratories (Wilmington, MA) and allowed to acclimate at Tolero's laboratory facility for 3 days. Rats were fasted (no food, but with water) for 12 hours prior to the dosing. Animals (3 per group) were dosed with TP-3654 by oral gavage at a dose of 40 mg/kg in a volume of 400µL per 10g of body weight. TP-3654 was formulated in a solution of 20% polysorbate 20. Animals dosed intravenously were heated under a heat lamp prior to dosing to allow vasodilatation and visualization of the tail vein. These animals were dosed with 2mg/kg of TP-3654 in a volume of 200µL per 10g of body weight. After injection, pressure was applied to the site for a few seconds to stop bleeding from the injection. Immediately after each animal received the full dose, time zero began and blood was collected at the following time points 1, 5, 25, and 30 minutes, and 1, 2, 4, 8, 24, and 48 hours post dose. At the designated time points, an empty 1 ml syringe was used to clear the contents of the jugular vein catheter that had been pre-loaded with heparin and discarded. A new empty syringe was used to draw 200µL of whole blood and the blood was immediately added to EDTA-coated tubes with the appropriate labels. The tubes were gently shaken to ensure the entire volume of blood interacted with the EDTA to avoid clotting. The

collected blood was stored on ice until centrifugation and cryo-storage of plasma. A third syringe containing heparin was used to reload the catheter to prevent clotting. After the blood was collected it was centrifuged at 5000 rpm for 5 minutes at 4°C. The plasma layer was removed and stored at -80°C until extraction and analysis. These steps were repeated until all time points in the study were collected and properly stored. Plasma samples were extracted using standard techniques and analyzed by LC-MS to quantify TP-3654 concentrations. Pharmacokinetic parameters were determined using the PKSolver add-in program for Excel.

Results

A second generation PIM kinase inhibitor, TP-3654 (Fig. 1.1A), was discovered as a lead candidate based on improved potency against PIM-1 and PIM-2 and decreased hERG activity *in vitro* as compared to SGI-1776. TP-3654 was tested against a panel of 340 kinases at 1 μ M, and inhibited 38 kinases by >50%. IC₅₀ determinations of 38 protein kinases and 4 additional lipid kinases (PI3K family) revealed 22 kinases with IC₅₀ values below 300 nM (Fig. 1.1B). TP-3654 displays at least 10-fold or greater selectivity for PIM-1 compared to any other kinase tested. One notable kinase family inhibited by TP-3654 was PI3K (γ , δ , and α), while selectivity against FLT3 was reduced by nearly 100-fold relative to SGI-1776 (Table 1.1).

The cellular potency of TP-3654 was determined by measuring its effect on baseline phosphorylation of BAD, a known substrate of PIM, on serine 112 by over-expression of PIM-1 and BAD in HEK-293 cells. Over-expression of the catalytically inactive mutant PIM-1 (K67M) did not increase phosphorylation of BAD compared to BAD transfection alone and was used as a negative control to subtract BAD phosphorylation by cellular kinases other than PIM-1. TP-3654 demonstrated potent PIM-1 specific cellular activity in the PIM-1/BAD over-expression system with an average EC₅₀ = 67 nM (Fig. 1.1C).

The over-expression models were helpful in establishing the anti-PIM activity of TP-3654. Translational models with more clinical relevance were explored for PIM dependency using shRNA knockdown. The UM-UC-3 urinary epithelial bladder carcinoma cell line was used to verify and validate dependency on PIM-1 for growth. PIM-1 mRNA was significantly reduced using two independent shRNAs targeting PIM-1 compared to the non-target shRNA control (Fig. 1.2A). Further, PIM-1 protein was reduced using PIM-1 shRNA compared to non-target shRNA, and 2D-colony growth was markedly reduced with PIM-1 knockdown (Fig. 1.2A), comparable to a previous report in the literature (40). Additionally, TP-3654 reduced colony growth of UM-UC-3 and PC-3 cells (Fig. 1.2B and 1.2C), confirming the PIM-1 dependent growth for both cell lines.

Additional bladder cancer cell lines were tested for levels of PIM-1, 2, and 3 (Fig 1.3b). Consistent with previous results, all 4 bladder cancer cell lines expressed high levels of PIM-1. The UM-UC3 cell line expressed the highest levels of PIM-1 and PIM-2 (Fig 1.3b) and was the most sensitive to TP-3654 in apoptosis assays (Fig 1.3a). For this reason, we continued our studies in the UM-UC3 cell line, focusing on PIM-1. PIM-1 siRNA knockdown or treatment with TP-3654 in UM-UC3 cells resulted in decreased levels of phosphorylated BAD (S112) (Fig 1.3c-d). To exclude the possibility that this pBAD decrease was due to off-target activity, we measured levels of p4EBP1 (decreased p4EBP1 is also seen in apoptotic conditions) in parallel with pBAD. We found no appreciable difference in levels of p4EBP1 in PIM-1 siRNA or TP-3654 treated cells (Fig 1.3c-d), providing further evidence that PIM inhibition was the primary reason for the pBAD decrease observed in TP-3654 treated cells and not activity of the compound inhibiting AKT, another kinase that phosphorylates BAD in certain conditions.

Because PIM kinases have been implicated in number of cancers including hematological

and prostate cancers (32, 33, 41-46), we sought to further evaluate PIM expression in low, high, non-invasive, and invasive bladder cancer cases. Evaluation of PIM expression by immunohistochemistry revealed a significant number of cases in which PIM was expressed in greater than 25% of the neoplastic cell population (Fig 1.4, Table 1.2). Low grade non-invasive tumors demonstrated the highest percentage of cases expressing PIM-1 (43%) and PIM-3 (52%) while invasive high grade lesions demonstrated the lowest percentage of PIM-1 (12%) and PIM-3 (13%) staining. PIM-2 was overexpressed in the majority of non-invasive high grade cases (63%) and in a significant minority of invasive high grade cases (38%) and non-invasive low grade cases (33%).

We next tested whether TP-3654 could inhibit the growth of established mouse xenograft tumors using the UM-UC-3 and PC-3 solid tumor cell lines that were tested *in vitro*. Oral dosing of 200 mg/kg of TP-3654 significantly reduced both UM-UC-3 and PC-3 tumor growth measured by volume (caliper) and by final tumor weight, with no significant changes in body weight or gross adverse toxicity (Fig. 1.5).

Previous studies showed that SGI-1776 exhibited favorable pharmacokinetic properties. We therefore sought to determine if TP-3654 retained or possibly improved upon the pharmacokinetic parameters of SGI-1776. A pharmacokinetic study in female rats was carried out as described in the materials and methods section. Rats were orally dosed with TP-3654 formulated in 20% polysorbate 20 and compared to intravenous injected control (Fig 1.6). This formulation showed favorable oral bioavailability at 39%. Using this formulation the T_{max} for TP-3654 was 1 hour with a half-life of 4.1 hours (Fig 1.6).

Discussion

PIM kinases play central roles in tumor cell survival and protection from apoptosis,

implicating this family of kinases as valid therapeutic targets (16-19). To date, numerous inhibitors of PIM kinases have been generated which exhibit growth suppressive activity in tumor cell line models *in vitro* and *in vivo* (9, 11, 14, 17, 19, 25, 48, 49). Previous PIM kinase inhibitors demonstrated antitumor activity in xenograft models of FLT3-ITD mutant AML and renal cell carcinoma (32, 43-47). We have developed a novel small molecule PIM kinase inhibitor that reduces the growth of solid tumor xenografts where the tumorigenicity is mediated by over-expression of PIM-1 or PIM-2, as well as human bladder carcinoma tumors. The combination of inhibiting all three PIM family members together in one compound may promote the observed antitumor activity.

Although the expression and activity of PIM kinases are well characterized in AML and prostate cancers, we sought to further evaluate the role of PIM kinases in bladder carcinomas. Previous work evaluating bladder carcinoma indicated that PIM-1 was expressed in over 80% of malignant tissues compared with normal epithelia, and expression was enhanced when comparing specimens derived from bladder cancer patients with invasive versus non-invasive tumors (40). Further, it was shown that shRNA knockdown of PIM-1 in bladder carcinoma cell lines reduced the growth of the cells *in vitro*, indicating a prominent role for PIM-1 in bladder carcinoma (40). We evaluated TP-3654 in the bladder cancer model UM-UC-3 *in vitro* and showed that the compound was able to induce similar effects as PIM-1 shRNA/siRNA mediated knockdown (Fig 1.2a-c, Fig 1.3c-d).

In addition to the *in vitro* data, examination of surgical resection cases of urothelial carcinoma revealed PIM kinase expressed in a significant number of cases when evaluated by immunohistochemistry. There was significant variation across the different groups. Interestingly, PIM-1 and PIM-3 showed a much higher percentage of cases staining in low grade

non-invasive carcinoma as compared to invasive high grade urothelial carcinoma where only a small minority retained positive staining. PIM-2 in comparison was expressed highest in a majority of non-invasive high grade lesions and in more than one-third of invasive lesions suggesting PIM-2 expression remains important in more aggressive clinical disease. These findings suggest that expression of PIM kinases contributes to uncontrolled growth in low and high grade non-invasive carcinoma and a smaller number of high grade invasive tumors.

TP-3654 reduced the growth of established UM-UC-3 xenografts (Fig 1.5), further suggesting that PIM-1 over-expression in patient bladder tumors may be sensitive to perturbation. As our pharmacokinetic study was performed in rats, it is important to note that off-target activity may have played a role in the therapeutic effect seen in the mouse xenografts. Additional pharmacokinetic, xenograft, and *ex vivo* studies are needed to fully understand the potential benefits of PIM kinase inhibition in urothelial carcinomas.

The rationale for targeting PIM kinases for the development of cancer therapies includes their over-expression in a variety of malignancies, correlation of high expression levels with poor patient prognosis, their oncogenicity when over-expressed in cells, their role in tumor cell survival as demonstrated by expression knockdown in multiple cancer types, and the development of inhibitors with preclinical activity which are emerging as clinical agents (29, 37). Together, these data support the long-standing effort to generate a therapeutic platform from which to target this family of cell survival kinases. Although the initial clinical evaluation of SGI-1776 was halted due to a narrow therapeutic window, the significant potential for therapeutic application of improved drug candidates remains. Given the rapid pace of discovery, optimization and development of new PIM kinase inhibitors, one or more will likely gain momentum as a key part of the armamentarium of treatments for both solid and hematologic

malignancies, including urothelial carcinomas.

CHAPTER 2: Inhibition of PIM Kinases Results in Downregulation of Oncogenic CMYC Signaling and Induction of Apoptosis in Hematological Malignancies, Including Acute Myeloid Leukemia and Multiple Myeloma

Kent J. Carpenter

Department of Physiology and Developmental Biology, Brigham Young University, Provo, Utah
84602, USA

Abstract

The three PIM kinases, PIM-1, PIM-2, and PIM-3, are a subfamily of serine/threonine kinases that are known to be involved in signaling pathways as downstream effectors of signal transducer and activator of transcription-5 (STAT5) signaling and inhibitors of apoptosis. PIM kinases lack a regulatory domain and are largely controlled at the transcriptional level. PIM kinases are implicated in a large percentage of hematological malignancies and solid tumors. Because they have been shown to correlate with disease progression and poor prognosis in many of these conditions, PIM kinase inhibitors are being developed and investigated for therapeutic use. More recent studies have indicated that PIM-1 plays a role in the upregulation of oncogenic c-MYC signaling, a hallmark of many cancers.

The aim of this study was to investigate the effects of TP-3654 on the interaction of c-MYC with PIM kinase family members. The data indicate that PIM-1 only interacts with c-MYC in the AML and multiple myeloma (MM) cell lines studied, and that PIM-1 siRNA knockdown or treatment with TP-3654 is able to decrease this interaction. In addition, TP-3654 potently induced apoptosis in the AML and MM cell lines studied.

These results suggest that second-generation PIM kinase inhibitor TP-3654 is effective at inhibiting PIM kinases and their downstream target c-MYC. These results contribute to the growing body of evidence that PIM kinase inhibitors have therapeutic potential in AML and introduce them as a potential target in MM.

Introduction

Cancer continues to be a worldwide epidemic. Cancers have accounted for more than 10% of recorded deaths each year in the world every year since 2007. Global cancer rates are expected to rise due to an aging population and lifestyle changes in the developing world¹. Hematological malignancies account for approximately 9.5% of newly diagnosed cancers in the United States each year, and new treatments are needed to battle the problem of malignant cell resistance to common chemotherapeutics^{1,2}.

The serine/threonine family of PIM kinases were first identified as proto-oncogenes activated in T-cell lymphomas induced by murine leukemia viruses³. The PIM kinase family is comprised of 3 family members (PIM-1, PIM-2, and PIM-3) with six different isoforms from alternate translation initiating sites³⁻⁵. Although the PIM kinase family is transcriptionally and translationally regulated in cells, these kinases lack a regulatory domain and are constitutively activated when expressed³⁻⁵.

Expression of PIM-1 is induced by several cytokines, which often activate STAT5 in conjunction with PIM-1. In fact, the PIM kinases are target genes of STAT3 and STAT5 and are correlated with high levels of STAT signaling⁶. They often form complexes with Hsp70 and Hsp90 for stabilization, but are eventually polyubiquitinated for proteasomal degradation³⁻⁵.

Although they were first implicated in human AML cases, PIM kinases are over-expressed in many different types of malignancies including hematologic and solid tumors. Specifically, over-expression has been identified in bladder, prostate, head & neck, and other hematologic malignancies. Over-expression of PIM kinases is often associated with poor prognosis in each of these cancers⁷⁻⁹. Additional research suggests that targeting PIM kinases may be beneficial to halt disease progression in hematological malignancies where PIM kinases

are expressed, including AML, MM, and certain types of lymphomas^{2, 3, 10-14}.

The PIM kinases have a variety of downstream targets that are thought to contribute to tumor growth. In particular, PIM kinases target the pro-apoptotic Bcl2-associated death promoter (BAD) family members and inhibit apoptosis^{4-6, 13-15}. Inhibitors of PIM kinases have been developed and effectively induce apoptosis in AML, MM, prostate, bladder, and other cancer cell lines^{9, 16, 17}. These inhibitors are also able to restore sensitivity of resistant cell lines to some chemotherapeutics, such as cisplatin, because PIM kinases actively upregulate expression of the efflux transporters MDR-1 and BCRP^{9, 16, 17}.

In addition, it has been shown in prostate tumors that PIM-1 and c-MYC associate together, resulting in transcriptional up-regulation and stabilization of c-MYC. Such prostate tumors exhibited higher Gleason scores, indicating greater disease progression and poorer prognosis⁸. c-MYC is an important oncogenic transcription factor that is able to regulate gene expression through binding of enhancer box sequences and recruitment of histone acetyl transferases (HATs)^{3, 16}. The MYC gene was first discovered in Burkitt's lymphoma patients and is located on chromosome 8^{10, 11}. Like PIM kinases, c-MYC is highly expressed in many cancers, most notably hematological malignancies, where preliminary data has shown that PIM kinases are able to directly and indirectly activate c-MYC^{10, 11}.

PIM kinase inhibitors are currently in development with some in clinical trials because of their potential to inhibit disease progression and induce apoptosis in AML cells. Crystal structures for both PIM-1 and PIM-2 have been used to understand their unique ATP binding pocket and for computational and medicinal chemistry efforts to develop inhibitors. First generation PIM kinase inhibitor SGI-1776, developed by Astex Pharmaceuticals (formerly SuperGen Inc.), was evaluated in a phase I clinical trial recruiting patients with either prostate

cancer or non-Hodgkin's lymphoma¹⁶. Eventually, the trial was terminated due to a narrow therapeutic window due to inhibition of the cardiac potassium channel hERG (human Ether-à-go-go-Related Gene)^{9, 16}.

A second-generation PIM kinase inhibitor TP-3654, owned by Tolero Pharmaceuticals in Lehi, Utah, is under evaluation because it has less off target inhibition (FLT3 kinase activity) than SGI-1776 and no appreciable hERG inhibition. TP-3654 was the primary PIM kinase inhibitor used in these studies.

The aim of this study was to further evaluate the association of PIM kinases with c-MYC in acute myeloid leukemia (AML) and multiple myeloma (MM) cell lines, where higher expression of PIM kinases has been associated with disease progression and poor prognosis.

Materials and Methods

Synthesis of TP-3654

TP-3654 was obtained from Tolero Pharmaceuticals Inc., currently located in Lehi, UT. TP-3654 (4-((3-(3-(Trifluoromethyl)phenyl)imidazo[1,2-b]pyridazin-6-yl)amino) -*trans*-cyclohexyl)propan-2-ol) was prepared according to United States Patent Application Publication US2012/0058997 (Imidazo[1,2-B]pyridazine and pyrazolo[1,5-A]pyrimidine derivatives and their use as protein kinase inhibitors).

Cell Lines

Cell lines were obtained from the American Type Culture Collection (ATCC) agency located in Manassas, Virginia. Cells were cultured in 75mL flasks in 10% fetal bovine serum (FBS) supplemented media. Each cell line was grown in the media recommended on the website of ATCC.

Cell Lysis and Western Blots

In all applications, cells were washed with cold PBS, treated with cell lysis solution (Cell Signaling), and then scraped when applicable. Lysates were centrifuged at 14,000g at 4°C and the supernatant used for protein quantification, according to the protocol. Protein levels were measured and normalized using the BCA Protein Assay (Pierce). Normalized amounts of lysate in electrophoresis buffer were then boiled and run on pre-cast gels according to the manufacturer protocol, using MOPS running solution (Invitrogen). Gels were transferred using the iBlot system (Invitrogen) and then blocked for one hour in 5% non-fat dry milk TBS-tween (TBST) solution. Blots were treated with specified antibodies (all provided by Cell Signaling) diluted 1:1000 in 5% bovine serum albumin (BSA)-TBST solution separately on a blot shaker overnight at 4°C. Blots were rinsed 3 times for 5 minutes each after antibody treatments, according to the protocol. The blots were treated with rabbit secondary antibody solutions (Cell Signaling) for 1 hour at room temperature diluted 1:1000 in a 5% non-fat dry milk (NFDM) TBST solution. As with the primary antibodies, the blots were rinsed 3 times for 5 minutes each before imaging with an ECL kit.

Apoptosis Assays

For the AML and MM cell lines, drug treated cells were analyzed for apoptosis by measuring the expression of cleaved caspase-3, rather than flow cytometry. In this case, cells were lysed and analyzed for caspase-3 expression by Western blot, as described previously. Cells were seeded at 1×10^6 million cells per well in 6-well plates and drug treated immediately. Cells were incubated in the presence or absence of TP-3654 for 24 hours prior to lysis and analysis of caspase-3 expression.

PIM-1 siRNA

MV4-11 cells were transfected with 75pmol of PIM-1 or control siRNA using 6 or 9 μ L of Lipofectamine 2000 reagent (Invitrogen) diluted in Opti-MEM according to the protocol. Cells were treated with siRNA and transfection reagent for 24 hours before cell lysis, as described above. Levels of PIM-1 were analyzed by Western blot (Fig 2.2a) to confirm knockdown.

TP-3654 Immunoprecipitation Treatment

For the MV4-11 (AML) and ARP-1 (MM) cell line drug treatments, 2x10⁶ cells were placed in suspension culture in 6 well plates and drug treated at the specified concentrations at the same time. Cells were incubated with the drug for 12 hours before lysis. The lysates were then analyzed for immunoprecipitation as described below.

Immunoprecipitation

The interaction of PIM kinases and c-MYC in AML and MM cell lines was evaluated by immunoprecipitation (IP). Cell lysates were prepared and protein levels quantified as described previously. For each sample, enough lysate was added to obtain 200 μ g of total protein in 1mL of cell lysis solution, according to the protocol from Santa Cruz Biotechnology. 10 μ L of primary antibodies optimized for IP (Santa Cruz Biotechnology) were added and the lysates incubated for 1hr at 4°C. After the hour incubation, 20 μ L of G-protein agarose beads (Santa Cruz Biotechnology) were added to each sample followed by overnight incubation at 4°C. The following day, samples were spun at 5000rpm at 4°C to pellet the beads, according to the protocol. Beads were then washed with 1mL of cold phosphate buffered saline (PBS) solution. The wash was repeated 4 times before the beads were resuspended in electrophoresis buffer (Invitrogen). The resuspended beads were then boiled and run on SDS-PAGE gels as described for Western blots previously. Blots were incubated with cMYC primary antibody optimized for

Western blotting (Santa Cruz Biotechnology) at 1:200 in 5% BSA, TBST as described previously for Western blots. Mouse secondary antibody (Pierce) was used after overnight incubation at 1:5000 in 5% NFDN TBST solution for an hour at room temperature. Blots were washed after each antibody incubation step as described previously. For the MV4-11, KASUMI-1, and ARP-1 cell lines, lysates treated with beads alone and lysates treated with AXL+beads (the AXL protein does not interact with cMYC) were used as negative controls (Fig 2.1a-c lanes 1-2). Lysates were treated with cMYC antibody for both the IP and blotting steps as a positive control (Fig 2.1a-c lanes 3).

Results

In the MV4-11 and KASUMI-1 AML cell lines and the ARP-1 MM cell line, expression of PIM-1, 2, and 3 was evaluated. Consistent with previous results, PIM-1 was expressed in all the cell lines studied and PIM 1, 2, and 3 was expressed in the MV4-11 cell line (Fig 2.1a). This is likely the reason that the MV4-11 cell line was more sensitive to TP-3654 (Fig 2.3). In all 3 cell lines studied, PIM-1 alone interacted with cMYC (Fig 2.1b-d). This finding is most significant in the MV4-11 cell line, where PIM-1, 2 and 3 are highly expressed (Fig 2.1b). As TP-3654 is a potent PIM-1 inhibitor (Table 1.1), we expected that TP-3654 treatment would decrease the PIM-1-cMYC interaction observed in these cell lines. These results provide evidence that TP-3654 does decrease this interaction (Fig 2.2b,c). Additionally, when MV4-11 cells were treated with PIM-1 siRNA, the PIM-1-cMYC interaction was eliminated almost entirely (Fig 2.2a).

Discussion

In addition to our previous work in urothelial carcinomas, we sought to evaluate the role of PIM-1's interaction with cMYC in AML and MM cell lines. Even though PIM 1, 2 and 3 was

expressed in the MV4-11 cell line (Fig 2.1a), PIM-1 alone interacted with cMYC in the same cell line (Fig 2.1b). This PIM-1-cMYC interaction was observed in the other cell lines studied (Fig 2.1c-d), and this interaction was decreased within 12 hours of TP-3654 treatment (Fig 2.2b-c).

As a transcription factor, cMYC is a very difficult drug target in spite of the fact that it is upregulated in many different types of cancers. These findings suggest that inhibition of PIM kinases may present a way to indirectly decrease cMYC signaling. Further studies, including chromatin immunoprecipitation (ChIP) analysis of downstream targets of cMYC are currently underway to further analyze the effects of PIM kinase inhibition in AML and MM cells.

The rationale for targeting PIM kinases includes their over-expression in solid tumors and hematological malignancies, their frequent correlation with poor prognosis, their role in inhibition of apoptosis, and their oncogenicity when over-expressed in cells. In fact, PIM kinase inhibitors are already in clinical trials and additional drug candidates are being explored. It is clear that TP-3654 or other PIM kinase inhibitors will likely become a key part of the armamentarium of treatments for both solid and hematological malignancies.

CHAPTER 3: Inhibition of The Tyrosine Kinase Receptor AXL Blocks Cell Invasion and Promotes Apoptosis in Pancreatic Cancer Cells

Kent Carpenter¹, Alexis Mollard², Lee Call³, Jared Bearss², Hariprasad Vankayalapati², Sunil Sharma², Mark Wade², Marc D Hansen¹, Steven L Warner³, and David J Bearss^{1,3}

Authors Affiliation: 1. Department of Physiology and Developmental Biology, BYU, Provo, UT. 2. Huntsman Cancer Institute, University of Utah, Salt Lake City, UT. 3. Tolero Pharmaceuticals, Inc., Salt Lake City, UT.

Abstract

Pancreatic cancer is virtually a uniformly lethal disease and a better understanding of the molecular basis of this malignancy is needed to discover new ways to prevent or treat this deadly disease. A central feature of malignant cells is their ability to disseminate from the primary tumor and establish local and distant metastases. In most cases, cancer patients with localized disease have significantly better prognosis than those with metastatic tumors and the majority of cancer mortality is associated with metastatic disease rather than the primary tumor. The receptor tyrosine kinase Axl is overexpressed in over 50% of pancreatic cancers and expression of Axl in these cancers is highly associated with a poor prognostic outcome for patients. Axl is a TAM family receptor tyrosine kinase involved in multiple aspects of tumorigenesis. Increased expression of Axl is associated with increased oncogenic transformation, cell survival, proliferation, migration, angiogenesis, and cellular adhesion. The known ligand for Axl is the Growth Arrest Specific Gene-6 (Gas6) protein and its binding to Axl leads to Axl autophosphorylation and activation of downstream signaling pathways including MAPK and PI3K/Akt pathways. We discovered and developed a small molecule Axl kinase inhibitor, TP-0903, and explored it for the effectiveness of targeting the Axl kinase in cell-based models of pancreatic cancer. TP-0903 is a 2-((2,5-substitutedpyrimidin-4-yl)amino)-N,N-dimethyl benzene sulfonamide that has low nanomolar (IC₅₀ = 12 nM) activity against the Axl kinase in a biochemical assays. In further biochemical evaluation, TP-0903 was shown to inhibit the entire

TAM family of kinases (IC₅₀ Axl = 12 nM; IC₅₀ Mer = 60 nM; Tyro3 = 71% inhibition at 200 nM). TP-0903 inhibits a small number of additional kinases when screened in a kinase panel of over 500 kinases and has demonstrated an ADMET profile suggesting it may be a potential clinical candidate. In cell proliferation assays, TP-0903 significantly inhibited pancreatic cancer cell growth at concentrations as low as 30 nM. In pharmacodynamic assays, TP-0903 dramatically inhibited Akt signaling (pAKT S473) downstream of GAS6 stimulation in pancreatic cancer cell lines. Consistent with the known function of Axl, TP-0903 inhibited Gas6-induced migration and invasion of pancreatic cancer cells in vitro and potently induces apoptosis. Mechanistically, TP-0903 decreases the expression of genes involved in Epithelial-Mesenchymal Transition (EMT) and induces cells to take on more epithelial phenotypes. TP-0903 also significantly inhibited the growth of pancreatic cancer cell lines grown in xenograft tumor mouse model and taken together, these results suggest Axl is a potential therapeutic target in pancreatic cancer and TP-0903 as a potential therapeutic agent.

Introduction

Pancreatic cancer is a deadly disease characterized by high levels of malignant, metastatic cells that have a high capacity to disseminate from the primary tumor and invade other tissues (50-52). This metastatic progression is enhanced by tumor cell activation of epithelial-to-mesenchymal transition (EMT), a developmental program in which epithelial cells assume a mesenchymal phenotype during gastrulation and organogenesis, allowing single cell invasive movement away from the ectodermal layer. EMT in cancer cells is associated with the acquisition of many stem cell-like features and immunosuppression that cooperatively support metastasis (53-56). The search for critical regulators of metastatic progression has focused on proteins that promote EMT and provide signals that support cell migration and invasion. One

such protein is the receptor tyrosine kinase Axl (57-59).

Axl belongs to the subfamily of RTKs called the TAM receptors. This subfamily includes Axl, Tyro3 and Mer (59-64). The TAM receptors are defined by a combination of two immunoglobulin-like domains and dual fibronectin type III repeats in the extracellular region of the protein. Two ligands, Gas6 (growth arrest-specific 6) and protein S have been identified for the TAM receptors. These ligands are vitamin K-dependent proteins that exhibit 43% amino-acid sequence identity and share similar domain structures (59-64). These proteins have a N-terminal Gla domain containing 11 γ -carboxyglutamic acid residues followed by four epidermal growth factor-like modules and a C-terminal sex hormone-binding globulin (SHBG)-like structure consisting of two tandem laminin G domains. The SHBG domain is both necessary and sufficient for TAM receptor binding and activation, whereas the Gla domain binds the negatively charged membrane phospholipids and plays an important role in TAM-mediated phagocytosis of apoptotic cells (59, 60, 70-75).

Axl was originally cloned from patients with chronic myelogenous leukemia and, when overexpressed, it exhibits transforming potential (70-73). Axl overexpression has been reported in a variety of human cancers including metastatic pancreatic cancer, colon cancer, thyroid carcinoma, breast cancer and pancreatic cancer. Axl is highly expressed in metastatic prostate cancer cells compared with normal prostate cells and other prostatic carcinoma cell lines (75-77). Inhibition of Axl signaling by a dominant-negative receptor mutant (AXL-DN) suppresses experimental gliomagenesis, migration and invasion, and leads to long-term survival of mice after intracerebral glioma cell implantation compared with Axl wild-type transfected tumor cells (78, 79). Additionally, Axl is detected at higher levels in metastases or malignant tumors than in normal tissues or primary tumors, and a higher level is associated with a poor clinical outcome

(50, 55, 79-82).

Axl seems to play two critical roles in cancer cells. First as a transforming gene that is overexpressed in human tumors, and secondly as a key mediator of the Gas6/Axl signaling system that is activated in the vasculature (80-85). Unlike many RTK oncoproteins, Axl can transform fibroblasts even in the absence of ligand (85-88). Therefore, Axl activation may be mediated through dual mechanisms that can involve interaction of Axl with its endogenous ligand, Gas6 as well as GAS6 independent activation (88-92). The Gas6/Axl system has been shown to play an important role in vascular biology. GAS6/Axl signaling promotes cell growth, antiapoptosis and migration in vascular smooth muscle cells, endothelial cells and fibroblasts (92-95). Recent studies also indicate that Gas6/Axl signaling affects multiple cellular behaviors required for neovascularization and maintaining vascular integrity (92, 94). These findings indicate that Axl regulates processes fundamental for both tumorigenesis and angiogenesis.

It was recently reported that Axl is aberrantly expressed in over 50% of pancreatic cancers and expression of Axl in pancreatic cancers confers an adverse prognostic influence (50, 59, 99). We have developed small molecule inhibitors that target Axl kinase activity and block downstream signaling from the activated receptor. These compounds display activity in the low nanomolar range and have been optimized to exhibit properties consistent with drug-like clinical candidates. One compound, TP-0903, exhibits potent AXL inhibition in the low nanomolar range and is currently being investigated for its clinical potential in pancreatic cancer.

Using established pancreatic cancer cell lines, we sought to evaluate the effects of TP-0903 treatment on these cells. Overall, the data presented here suggest that inhibition of AXL with TP-0903 results in suppression of EMT marker genes, decreased cell migration, and induction of apoptosis in the pancreatic cancer cell lines studied.

Materials and Methods

Biochemical Assays

Biochemical kinase assays were utilized to determine IC50 values for TP-0903 against these four kinases. Reactions were run using Invitrogen's TR-FRET LanthaScreen assay and using ATP concentrations at the apparent Km for each kinase.

pAKT ELISA

Pancreatic cancer cell lines (PSN-1 and PL45) were serum starved overnight, treated for 2 hours with TP-0903, and stimulated with Gas6 for 5 minutes. Lysates from these cells were analyzed for total-Akt and phospho-Akt (Ser473) using the Meso Scale Discovery platform.

Migration Assays

In order to test for a role of AXL in cell migration, TP-0903 was applied to a panel of cancer cell lines and migration measured. The cell line panel included a series of 8 pancreatic cell lines and a breast cancer cell line, MDA-MB-XXX, with high AXL expression. Cells were seeded onto collagen-coated wells of the Platypus Oris system, where a barrier prevents cells from accessing the center of the well. After overnight culture, the barrier is removed, drug (5uM) is applied from DMSO stocks and the cells are cultured for 16 hours to allow migration into the open area of the well plate. Importantly, cells are grown in 10% serum conditions, conditions that result in saturated activation of AXL signaling.

Apoptosis Assays

We assessed TP-0903's ability to induce apoptosis in the PANC-1 and PSN-1 cell lines using the violet radiometric membrane asymmetry probe/dead cell apoptosis kit for flow cytometry kit from Invitrogen. Cells were seeded in 6-well plates at a concentration of 250,000 cells per well,

allowed to grow for 48 hours, and then drug treated with the specified concentrations of TP-0903 for 24 hours. Dyes were added and measured on the flow cytometer and gates were set according to the protocol. Cells were treated with 10 μ M cisplatin for 24 hours in the same manner as above for use as a positive control.

Real Time PCR

Quantitative PCR analysis was performed using the StepOne Plus Real-time PCR system from Life Technologies Inc. Cells were first seeded at a concentration of 250,000 cells per well in 6 well plates, allowed to grow for 6 hours, and then treated with specified concentrations of TP-0903 for 2 hours prior to RNA isolation. RNA isolation was carried out using the RNeasy kit (QIAGEN) according to the protocol, including treatment with the RNase-free DNase set from the manufacturer. RNA levels were normalized using a nanodrop spectrophotometer (Life Technologies). RT and PCR reactions were carried out using the SYBR-Green One Step RNA to Ct kit (Life Technologies) according to the protocol for 20 μ L reactions. Commercially available primers (QIAGEN Quantitect Primer Assays) were used to target the EMT genes Snail, Twist, E-cadherin, and AXL. Reactions for each EMT gene target were carried out in triplicate while the 18S loading controls were carried out in quadruplicate. Δ CT values were determined by subtracting each treatment group from its corresponding 18S CT average. Δ Δ CT reactions were determined by subtracting each drug treated group from the vehicle treated control groups. Relative quantification was then determined from the Δ CT values. The data shown are the averages from two independent experiments, both carried out in the same manner as described above, with error bars denoting the standard error of the mean in each case.

Western Blots

Western blots were carried out to confirm real-time PCR results. Both the PSN-1 and PANC-1

cell lines were again seeded in 6 well plates at a concentration of 250,000 cells per well, allowed to grow for 6 hours, and then treated with varying concentrations of TP-0903. Cell lysis was carried out 24 hours later using a standard cell lysis kit (Cell Signaling Technologies). Protein levels were measured using the BCA protein assay (Pierce) according to the protocol. Lysates were then normalized and run on pre-cast gels (Invitrogen) according to the Invitrogen protocol. Gels were transferred using the iBlot system also available from Invitrogen. Blots blocked for 1 hour at room temperature in a 5% non-fat dry milk (NFDM) solution before leaving overnight at 4°C in antibody solutions. Antibody solutions (Cell Signaling Technologies) were prepared in a 5% bovine serum albumin (BSA) solution and diluted 1:1000. The next day, blots were treated with the corresponding secondary antibodies for 1 hour at room temperature in a 5% NFDM solution before imaging using a Western ECL detection kit.

Soluble AXL Data

Serum samples from cancer patients were evaluated for sAxl levels. The results indicate a statistically significant difference between the mean of the control (CTL) group and the PDA (panc) group ($p < 0.05$). Furthermore, there appears to be a subgroup of colon, lung, and PDA patients with particularly high sAxl levels.

Xenograft Study

PSN-1 cells were implanted subcutaneously in mice and allowed to establish tumors. TP-0903 was orally administered to the mice daily (M-F) for three weeks. Tumor and body weight measurements were taken twice a week.

Pharmacokinetic Data

Mice were dosed orally with 50 mg/kg TP-0903 and blood was collected at the indicated time

points. Plasma samples were analyzed by mass spectrometry and standard PK parameters were calculated from these data.

Results

TP-0903 is a Multi-Targeted Kinase Inhibitor With Potent Activity Against AXL

Our second-generation AXL inhibitor, TP-0903, was developed as an analogue to first generation AXL inhibitor SGI-7079. Compared with SGI-7079, TP-0903 displays significantly greater AXL inhibition at lower nanomolar concentrations (Fig 3.1).

Migration Assays

In these experiments different cell lines exhibit different rates of migration, as determined by the amount of space covered by cells at the end of the experiment. In almost all cell lines tested, a reduction in the amount of migration is observed. The observation is born out by statistical analysis of the data sets for drug-treated and control conditions for each cell line; 6 of 9 cell lines showing a statistically-significant reduction in cell migration by student t-test (Fig 3.3).

TP-0903 Potently Induces Apoptosis in Pancreatic Cancer Cell Lines

In addition to our migration assays, we sought to determine which concentrations TP-0903 was able to induce apoptosis in the pancreatic cancer cell lines studied. We found TP-0903 to significantly induce apoptosis in both the PANC1 and PSN-1 cell lines within 24 hours. TP-0903 induced apoptosis at significantly higher levels at lower concentrations than our cisplatin-treated positive controls (Fig 3.4).

AXL Inhibition by TP-0903 Significantly Reduces Expression of EMT Marker Genes

To further confirm our migration assay results, we sought to determine the effects of

AXL inhibition with TP-0903 on EMT marker gene expression using the same two pancreatic cancer cell lines PANC1 and PSN-1. First, the pancreatic cancer cell lines were treated with TP-0903 in 6-well plates and their expression of EMT genes slug, snail, twist, and E-cadherin by real-time PCR and Western blot analysis. For real-time PCR analysis, cells were treated with drug for only 2 hours to avoid any potential apoptotic or dead cell interference in measuring RNA levels. In both pancreatic cancer cell lines studied, we found that TP-0903 treated cells expressed significantly less snail and twist (Fig 3.5a-b). As expected, E-cadherin levels increased in each case relative to the vehicle-treated cells in a concentration-dependent manner (Fig 3.5a-b). It is not clear, however, why lower concentrations of TP-0903 induced higher E-cadherin expression compared to higher concentrations of TP-0903.

Western blot analysis of the EMT marker genes snail, slug, and E-cadherin showed a similar trend (Fig 3.5c-d) for both cell lines studied. In this case, cells were treated in 6-well plates as with the qPCR, but were treated for 24 hours to allow for a change in protein levels.

sAXL in Pancreatic Cancer

In order to understand the role of sAxl in cancer we have used an Axl ELISA on conditioned media to detect sAxl levels quantitatively. In parallel, we have also evaluated Axl mRNA expression by RT-PCR and Axl RTK protein expression by western blot (Figure 3.6A-B). Interestingly, levels of Axl mRNA and sAxl were fairly well correlated ($r^2 = 0.61$). Similarly, protein levels as determined by western blot also showed good correlation with sAxl levels. For example, the cell lines PL45, BxPC3, and HPAC had high levels of Axl protein expression and were also among the highest for sAxl. HPAFII and Hs700T had the lowest expression of both Axl protein and sAxl. These data suggest that in at least PDA cell lines, sAxl may serve as a surrogate marker for monitoring the level of total Axl in the cancer cells. This finding may

translate to the pancreatic cancer patient allowing a simple blood test evaluating sAxl levels to predict patients with high levels of Axl in their tumors.

To determine if we can detect differential expression of sAxl in the serum of cancer patients, we evaluated serum from a panel of breast (10), colorectal (10), lung (10), and pancreatic (16) cancers using the Axl ELISA (Figure 3.6C). We also included serum from 23 individuals without cancer. There was significant overlap between the cancer groups and the normal serum group, but the normal group did not have a single individual over the 40 ng/ml level; whereas, a significant portion of the serum from cancer patients had sAxl levels higher than 40 ng/ml. Serum from PDA patients had sAxl levels as high as 66 and 78 ng/ml. These preliminary data suggest a subset of cancer patients with high levels of sAxl. To see if high sAxl correlated with favorable or poor prognosis, we compared these data to the overall survival of these cancer patients (lung and pancreas only). Two groups were created from the sAxl data. The first group consisted of the patients with high sAxl ($n = 4$) and the second group included patients with lower sAxl levels ($n = 22$). Although this data set is small (particularly the high sAxl group), we saw an interesting positive correlation between sAxl levels and overall survival. In other words, the few patients with the highest sAxl levels had the greatest overall survival.

TP-0903 Reduces Tumor Volume in Pancreatic Cancer Xenografts

In vivo xenograft studies of PSN-1 pancreatic cancer cells showed a significant reduction in tumor volume ($p < 0.001$) but an insignificant decrease in overall body weight ($p > 0.1$) by Student's t-test (Fig 3.7 A, B). Pharmacokinetic studies indicated favorable bioavailability (Fig 3.7 C).

Discussion

Progress has been made in the treatment of pancreatic cancer in the past decade, but it is

still largely incurable and many patients respond poorly to treatment. There is a clear need to develop targeted therapies aimed to reduce the mesenchymal character of cancer cells in solid tumors that are prone to metastasis, including pancreatic cancer. The receptor tyrosine kinase AXL has been previously implicated in pancreatic cancer and is correlated with poor prognosis in these cases (52, 53, 100). Because of the clear role of AXL in EMT and metastatic pancreatic cancer, we sought to evaluate the ability of our second-generation AXL inhibitor, TP-0903, to block pancreatic cancer cell migration and invasiveness.

TP-0903 was generated as a second-generation AXL inhibitor following SGI-7079. Compared with SGI-7079, TP-0903 is far more potent against AXL and shows nanomolar inhibition and toxicity in a variety of cancer cell lines. In addition to its inhibition of cell growth, TP-0903 significantly reduced migration in 6 out of the 9 mesenchymal pancreatic cancer cell lines studied.

To clarify that these migration results were the result of a decreased EMT phenotype in the cancer cells, we further studied the effect of TP-0903 on EMT gene expression in those cell lines showing highest AXL expression from the cell-line array. Real-time PCR and Western blot results of the EMT genes slug, snail, and twist show that TP-0903 treatment caused the cells to become less mesenchymal. As expected, E-cadherin expression increased with higher drug treatment, indicating the cells had become more epithelial.

The benefit of treatment with TP-0903 may extend beyond a mesenchymal to epithelial transition in malignant cells. *In vitro*, TP-0903 potently induced apoptosis in those cell lines expressing the highest levels of AXL. Our *in vivo* PSN-1 cell line xenograft studies similarly showed a significant reduction in tumor volume. Taken together, these results suggest that highly metastatic, Axl-expressing pancreatic carcinomas may become less invasive and sensitive to

perturbation when treated with AXL inhibitors.

While the role of AXL in cancer cells is established, we sought to evaluate the role of soluble AXL (sAXL) in tumor progression and prognostic outcome. The activated GAS-6-AXL complex is frequently cleaved from the cell membrane and left in the serum of cancer patients. We first used cell line models and found a positive correlation between Axl mRNA and protein expression and media sAXL levels. This preliminary data suggested that sAXL levels could be used as a marker for total AXL levels in cancer cells and, subsequently, as a prognostic marker for cancer patients.

To evaluate this hypothesis, we next moved to an *ex vivo* model, evaluating the serum of a panel of breast, colorectal, lung, and pancreatic cancer patients for sAXL by ELISA. Serum from cancer-free individuals was included as a control. Many of these patients had high levels of sAXL, but these high levels did not necessarily correlate with poor prognosis. In fact, those patients with the highest sAXL had a slightly better prognosis than those with lower sAXL levels. It is important to note that the data set used consisted of only ten individuals, and that correlation may not hold true in a larger population size. However, it is clear that sAXL levels in cancer patients may not necessarily correlate with cellular Axl levels. It has been reported that Gas-6 induced activation of Axl often results in a cascade event in which the receptor becomes constitutively active. In other words, Axl is often activated in the absence of ligand. Because sAXL is only found in a complex with Gas-6, it may be that many cells in metastatic tumors express Axl that has not been activated by Gas-6 and cleaved.

The rationale for targeting Axl is borne out of the observation that pancreatic cancer patients with metastatic disease frequently have poorer prognosis than early-stage disease. This is true for many other cancers. For example, Axl has been shown as correlated with a

mesenchymal phenotype in breast cancer cells and poor prognosis in breast tumors expressing high levels of Axl (52). Similar results were seen in esophageal and hepatocellular carcinomas (32, 53). We report that TP-0903 is able to not only inhibit migration but also induce apoptosis at low concentrations in both *in vitro* and *in vivo* models of pancreatic cancer. Additionally, TP-0903 displays favorable oral pharmacokinetics in both rat and mouse models, further demonstrating the therapeutic potential of TP-0903 in pancreatic and other cancers with metastatic potential.

REFERENCES

1. Cuypers HT, Selten G, Quint W, Zijlstra M, Maandag ER, Boelens W, et al. Murine leukemia virus-induced T-cell lymphomagenesis: integration of proviruses in a distinct chromosomal region. *Cell*. 1984;37(1):141-50. PubMed PMID: 6327049.
2. Meeker TC, Nagarajan L, ar-Rushdi A, Rovera G, Huebner K, Croce CM. Characterization of the human PIM-1 gene: a putative proto-oncogene coding for a tissue specific member of the protein kinase family. *Oncogene research*. 1987;1(1):87-101. PubMed PMID: 3329711.
3. Breuer ML, Cuypers HT, Berns A. Evidence for the involvement of pim-2, a new common proviral insertion site, in progression of lymphomas. *The EMBO journal*. 1989;8(3):743-8. PubMed PMID: 2721500; PubMed Central PMCID: PMC400870.
4. Saris CJ, Domen J, Berns A. The pim-1 oncogene encodes two related protein-serine/threonine kinases by alternative initiation at AUG and CUG. *The EMBO journal*. 1991;10(3):655-64. PubMed PMID: 1825810; PubMed Central PMCID: PMC452698.
5. Ragoussis J, Senger G, Mockridge I, Sanseau P, Ruddy S, Dudley K, et al. A testis-expressed Zn finger gene (ZNF76) in human 6p21.3 centromeric to the MHC is closely linked to the human homolog of the t-complex gene tcp-11. *Genomics*. 1992;14(3):673-9. PubMed PMID: 1427894.
6. Feldman JD, Vician L, Crispino M, Tocco G, Marcheselli VL, Bazan NG, et al. KID-1, a protein kinase induced by depolarization in brain. *The Journal of biological chemistry*. 1998;273(26):16535-43. PubMed PMID: 9632723.
7. Matikainen S, Sareneva T, Ronni T, Lehtonen A, Koskinen PJ, Julkunen I. Interferon-alpha activates multiple STAT proteins and upregulates proliferation-associated IL-2Ralpha, c-myc, and pim-1 genes in human T cells. *Blood*. 1999;93(6):1980-91. PubMed PMID: 10068671.
8. Kottaridis PD, Gale RE, Frew ME, Harrison G, Langabeer SE, Belton AA, et al. The presence of a FLT3 internal tandem duplication in patients with acute myeloid leukemia (AML) adds important prognostic information to cytogenetic risk group and response to the first cycle of chemotherapy: analysis of 854 patients from the United Kingdom Medical Research Council AML 10 and 12 trials. *Blood*. 2001;98(6):1752-9. PubMed PMID: 11535508.
9. Mizuno K, Shirogane T, Shinohara A, Iwamatsu A, Hibi M, Hirano T. Regulation of Pim-1 by Hsp90. *Biochemical and biophysical research communications*. 2001;281(3):663-9. doi: 10.1006/bbrc.2001.4405. PubMed PMID: 11237709.
10. Pasqualucci L, Neumeister P, Goossens T, Nanjangud G, Chaganti RS, Kuppers R, et al. Hypermutation of multiple proto-oncogenes in B-cell diffuse large-cell lymphomas. *Nature*. 2001;412(6844):341-6. doi: 10.1038/35085588. PubMed PMID: 11460166.
11. Wang Z, Bhattacharya N, Weaver M, Petersen K, Meyer M, Gapter L, et al. Pim-1: a serine/threonine kinase with a role in cell survival, proliferation, differentiation and tumorigenesis. *Journal of veterinary science*. 2001;2(3):167-79. PubMed PMID: 12441685.
12. Mikkers H, Allen J, Knipscheer P, Romeijn L, Hart A, Vink E, et al. High-throughput retroviral tagging to identify components of specific signaling pathways in cancer. *Nature*

- genetics. 2002;32(1):153-9. doi: 10.1038/ng950. PubMed PMID: 12185366.
13. Zhu N, Ramirez LM, Lee RL, Magnuson NS, Bishop GA, Gold MR. CD40 signaling in B cells regulates the expression of the Pim-1 kinase via the NF-kappa B pathway. *Journal of immunology*. 2002;168(2):744-54. PubMed PMID: 11777968.
14. Fox CJ, Hammerman PS, Cinalli RM, Master SR, Chodosh LA, Thompson CB. The serine/threonine kinase Pim-2 is a transcriptionally regulated apoptotic inhibitor. *Genes & development*. 2003;17(15):1841-54. doi: 10.1101/gad.1105003. PubMed PMID: 12869584; PubMed Central PMCID: PMC196230.
15. Gaidano G, Pasqualucci L, Capello D, Berra E, Deambrogi C, Rossi D, et al. Aberrant somatic hypermutation in multiple subtypes of AIDS-associated non-Hodgkin lymphoma. *Blood*. 2003;102(5):1833-41. doi: 10.1182/blood-2002-11-3606. PubMed PMID: 12714522.
16. Qian KC, Wang L, Hickey ER, Studts J, Barringer K, Peng C, et al. Structural basis of constitutive activity and a unique nucleotide binding mode of human Pim-1 kinase. *The Journal of biological chemistry*. 2005;280(7):6130-7. doi: 10.1074/jbc.M409123200. PubMed PMID: 15525646.
17. Shay KP, Wang Z, Xing PX, McKenzie IF, Magnuson NS. Pim-1 kinase stability is regulated by heat shock proteins and the ubiquitin-proteasome pathway. *Molecular cancer research : MCR*. 2005;3(3):170-81. doi: 10.1158/1541-7786.MCR-04-0192. PubMed PMID: 15798097.
18. Adam M, Pogacic V, Bendit M, Chappuis R, Nawijn MC, Duyster J, et al. Targeting PIM kinases impairs survival of hematopoietic cells transformed by kinase inhibitor-sensitive and kinase inhibitor-resistant forms of Fms-like tyrosine kinase 3 and BCR/ABL. *Cancer research*. 2006;66(7):3828-35. doi: 10.1158/0008-5472.CAN-05-2309. PubMed PMID: 16585210.
19. Holder S, Zemskova M, Zhang C, Tabrizizad M, Bremer R, Neidigh JW, et al. Characterization of a potent and selective small-molecule inhibitor of the PIM1 kinase. *Molecular cancer therapeutics*. 2007;6(1):163-72. doi: 10.1158/1535-7163.MCT-06-0397. PubMed PMID: 17218638.
20. Pogacic V, Bullock AN, Fedorov O, Filippakopoulos P, Gasser C, Biondi A, et al. Structural analysis identifies imidazo[1,2-b]pyridazines as PIM kinase inhibitors with in vitro antileukemic activity. *Cancer research*. 2007;67(14):6916-24. doi: 10.1158/0008-5472.CAN-07-0320. PubMed PMID: 17638903.
21. Zippo A, De Robertis A, Serafini R, Oliviero S. PIM1-dependent phosphorylation of histone H3 at serine 10 is required for MYC-dependent transcriptional activation and oncogenic transformation. *Nature cell biology*. 2007;9(8):932-44. doi: 10.1038/ncb1618. PubMed PMID: 17643117.
22. Wierenga AT, Vellenga E, Schuringa JJ. Maximal STAT5-induced proliferation and self-renewal at intermediate STAT5 activity levels. *Molecular and cellular biology*. 2008;28(21):6668-80. doi: 10.1128/MCB.01025-08. PubMed PMID: 18779318; PubMed Central PMCID: PMC2573230.

23. Zhang Y, Wang Z, Li X, Magnuson NS. Pim kinase-dependent inhibition of c-Myc degradation. *Oncogene*. 2008;27(35):4809-19. doi: 10.1038/onc.2008.123. PubMed PMID: 18438430.
24. Beharry Z, Zemskova M, Mahajan S, Zhang F, Ma J, Xia Z, et al. Novel benzylidene-thiazolidine-2,4-diones inhibit Pim protein kinase activity and induce cell cycle arrest in leukemia and prostate cancer cells. *Molecular cancer therapeutics*. 2009;8(6):1473-83. doi: 10.1158/1535-7163.MCT-08-1037. PubMed PMID: 19509254; PubMed Central PMCID: PMC3415237.
25. Bullock AN, Russo S, Amos A, Pagano N, Bregman H, Debreczeni JE, et al. Crystal structure of the PIM2 kinase in complex with an organoruthenium inhibitor. *PloS one*. 2009;4(10):e7112. doi: 10.1371/journal.pone.0007112. PubMed PMID: 19841674; PubMed Central PMCID: PMC2743286.
26. Chen LS, Redkar S, Bearss D, Wierda WG, Gandhi V. Pim kinase inhibitor, SGI-1776, induces apoptosis in chronic lymphocytic leukemia cells. *Blood*. 2009;114(19):4150-7. doi: 10.1182/blood-2009-03-212852. PubMed PMID: 19734450; PubMed Central PMCID: PMC2774551.
27. Xia Z, Knaak C, Ma J, Beharry ZM, McInnes C, Wang W, et al. Synthesis and evaluation of novel inhibitors of Pim-1 and Pim-2 protein kinases. *Journal of medicinal chemistry*. 2009;52(1):74-86. doi: 10.1021/jm800937p. PubMed PMID: 19072652.
28. Anizon F, Shtil AA, Danilenko VN, Moreau P. Fighting tumor cell survival: advances in the design and evaluation of Pim inhibitors. *Current medicinal chemistry*. 2010;17(34):4114-33. PubMed PMID: 20939820.
29. Brault L, Gasser C, Bracher F, Huber K, Knapp S, Schwaller J. PIM serine/threonine kinases in the pathogenesis and therapy of hematologic malignancies and solid cancers. *Haematologica*. 2010;95(6):1004-15. doi: 10.3324/haematol.2009.017079. PubMed PMID: 20145274; PubMed Central PMCID: PMC2878801.
30. Chang M, Kanwar N, Feng E, Siu A, Liu X, Ma D, et al. PIM kinase inhibitors downregulate STAT3(Tyr705) phosphorylation. *Molecular cancer therapeutics*. 2010;9(9):2478-87. doi: 10.1158/1535-7163.MCT-10-0321. PubMed PMID: 20667852.
31. Santio NM, Vahakoski RL, Rainio EM, Sandholm JA, Virtanen SS, Prudhomme M, et al. Pim-selective inhibitor DHPCC-9 reveals Pim kinases as potent stimulators of cancer cell migration and invasion. *Molecular cancer*. 2010;9:279. doi: 10.1186/1476-4598-9-279. PubMed PMID: 20958956; PubMed Central PMCID: PMC2978147.
32. Kelly KR, Espitia CM, Taverna P, Choy G, Padmanabhan S, Nawrocki ST, et al. Targeting PIM kinase activity significantly augments the efficacy of cytarabine. *British journal of haematology*. 2012;156(1):129-32. doi: 10.1111/j.1365-2141.2011.08792.x. PubMed PMID: 21689092.
33. Hospital MA, Green AS, Lacombe C, Mayeux P, Bouscary D, Tamburini J. The FLT3 and Pim kinases inhibitor SGI-1776 preferentially target FLT3-ITD AML cells. *Blood*.

- 2012;119(7):1791-2. doi: 10.1182/blood-2011-11-393066. PubMed PMID: 22343664.
34. Chen LS, Redkar S, Taverna P, Cortes JE, Gandhi V. Mechanisms of cytotoxicity to Pim kinase inhibitor, SGI-1776, in acute myeloid leukemia. *Blood*. 2011;118(3):693-702. doi: 10.1182/blood-2010-12-323022. PubMed PMID: 21628411; PubMed Central PMCID: PMC3142906.
35. Isaac M, Siu A, Jongstra J. The oncogenic PIM kinase family regulates drug resistance through multiple mechanisms. *Drug resistance updates : reviews and commentaries in antimicrobial and anticancer chemotherapy*. 2011;14(4-5):203-11. doi: 10.1016/j.drup.2011.04.002. PubMed PMID: 21601509.
36. Mahalingam D, Espitia CM, Medina EC, Esquivel JA, 2nd, Kelly KR, Bearss D, et al. Targeting PIM kinase enhances the activity of sunitinib in renal cell carcinoma. *British journal of cancer*. 2011;105(10):1563-73. doi: 10.1038/bjc.2011.426. PubMed PMID: 22015557; PubMed Central PMCID: PMC3242528.
37. Nawijn MC, Alendar A, Berns A. For better or for worse: the role of Pim oncogenes in tumorigenesis. *Nature reviews Cancer*. 2011;11(1):23-34. doi: 10.1038/nrc2986. PubMed PMID: 21150935.
38. Nishiguchi GA, Atallah G, Bellamacina C, Burger MT, Ding Y, Feucht PH, et al. Discovery of novel 3,5-disubstituted indole derivatives as potent inhibitors of Pim-1, Pim-2, and Pim-3 protein kinases. *Bioorganic & medicinal chemistry letters*. 2011;21(21):6366-9. doi: 10.1016/j.bmcl.2011.08.105. PubMed PMID: 21945284.
39. Siu A, Virtanen C, Jongstra J. PIM kinase isoform specific regulation of MIG6 expression and EGFR signaling in prostate cancer cells. *Oncotarget*. 2011;2(12):1134-44. PubMed PMID: 22193779; PubMed Central PMCID: PMC3282072.
40. Guo S, Mao X, Chen J, Huang B, Jin C, Xu Z, et al. Overexpression of Pim-1 in bladder cancer. *Journal of experimental & clinical cancer research : CR*. 2010;29:161. doi: 10.1186/1756-9966-29-161. PubMed PMID: 21143989; PubMed Central PMCID: PMC3012037.
41. Alvarado Y, Giles FJ, Swords RT. The PIM kinases in hematological cancers. *Expert review of hematology*. 2012;5(1):81-96. doi: 10.1586/ehm.11.69. PubMed PMID: 22272708.
42. Fathi AT, Arowojolu O, Swinnen I, Sato T, Rajkhowa T, Small D, et al. A potential therapeutic target for FLT3-ITD AML: PIM1 kinase. *Leukemia research*. 2012;36(2):224-31. doi: 10.1016/j.leukres.2011.07.011. PubMed PMID: 21802138; PubMed Central PMCID: PMC3380375.
43. Johrer K, Obkircher M, Neureiter D, Parteli J, Zelle-Rieser C, Maizner E, et al. Antimyeloma activity of the sesquiterpene lactone cnicin: impact on Pim-2 kinase as a novel therapeutic target. *Journal of molecular medicine*. 2012;90(6):681-93. doi: 10.1007/s00109-011-0848-x. PubMed PMID: 22205266.
44. Song JH, Kraft AS. Pim kinase inhibitors sensitize prostate cancer cells to apoptosis

triggered by Bcl-2 family inhibitor ABT-737. *Cancer research*. 2012;72(1):294-303. doi: 10.1158/0008-5472.CAN-11-3240. PubMed PMID: 22080570; PubMed Central PMCID: PMC3251634.

45. Tsuganezawa K, Watanabe H, Parker L, Yuki H, Taruya S, Nakagawa Y, et al. A novel Pim-1 kinase inhibitor targeting residues that bind the substrate peptide. *Journal of molecular biology*. 2012;417(3):240-52. doi: 10.1016/j.jmb.2012.01.036. PubMed PMID: 22306408.

46. Tshako AL, Brown DS, Koltun ES, Aay N, Arcalas A, Chan V, et al. The design, synthesis, and biological evaluation of PIM kinase inhibitors. *Bioorganic & medicinal chemistry letters*. 2012;22(11):3732-8. doi: 10.1016/j.bmcl.2012.04.025. PubMed PMID: 22542012.

47. Pierre F, Regan CF, Chevrel MC, Siddiqui-Jain A, Macalino D, Streiner N, et al. Novel potent dual inhibitors of CK2 and Pim kinases with antiproliferative activity against cancer cells. *Bioorganic & medicinal chemistry letters*. 2012;22(9):3327-31. doi: 10.1016/j.bmcl.2012.02.099. PubMed PMID: 22460033.

48. Bullock AN, Debreczeni J, Amos AL, Knapp S, Turk BE. Structure and substrate specificity of the Pim-1 kinase. *The Journal of biological chemistry*. 2005;280(50):41675-82. doi: 10.1074/jbc.M510711200. PubMed PMID: 16227208.

49. Jacobs MD, Black J, Futer O, Swenson L, Hare B, Fleming M, et al. Pim-1 ligand-bound structures reveal the mechanism of serine/threonine kinase inhibition by LY294002. *The Journal of biological chemistry*. 2005;280(14):13728-34. doi: 10.1074/jbc.M413155200. PubMed PMID: 15657054.

50. Maitra A, Hruban RH. Pancreatic cancer. *Annu Rev Pathol*. 2008;3:157-88. Epub 2007/11/28. doi: 10.1146/annurev.pathmechdis.3.121806.154305. PubMed PMID: 18039136; PubMed Central PMCID: PMC2666336.

51. Takikita M, Altekruse S, Lynch CF, Goodman MT, Hernandez BY, Green M, et al. Associations between selected biomarkers and prognosis in a population-based pancreatic cancer tissue microarray. *Cancer Res*. 2009;69(7):2950-5. Epub 2009/03/12. doi: 0008-5472.CAN-08-3879 [pii] 10.1158/0008-5472.CAN-08-3879. PubMed PMID: 19276352; PubMed Central PMCID: PMC2711977.

52. Jemal A, Siegel R, Ward E, Hao Y, Xu J, Murray T, et al. Cancer statistics, 2008. *CA Cancer J Clin*. 2008;58(2):71-96. Epub 2008/02/22. doi: CA.2007.0010 [pii] 10.3322/CA.2007.0010. PubMed PMID: 18287387.

53. Nakano T, Tani M, Ishibashi Y, Kimura K, Park YB, Imaizumi N, et al. Biological properties and gene expression associated with metastatic potential of human osteosarcoma. *Clin Exp Metastasis*. 2003;20(7):665-74. Epub 2003/12/13. PubMed PMID: 14669798.

54. Finger EC, Giaccia AJ. Hypoxia, inflammation, and the tumor microenvironment in metastatic disease. *Cancer Metastasis Rev*. 2010;29(2):285-93. Epub 2010/04/16. doi: 10.1007/s10555-010-9224-5. PubMed PMID: 20393783.

55. Craven RJ, Xu LH, Weiner TM, Fridell YW, Dent GA, Srivastava S, et al. Receptor tyrosine kinases expressed in metastatic colon cancer. *Int J Cancer*. 1995;60(6):791-7. Epub 1995/03/16. PubMed PMID: 7896447.
56. Pierreux CE, Cordi S, Hick AC, Achouri Y, Ruiz de Almodovar C, Prevot PP, et al. Epithelial: Endothelial cross-talk regulates exocrine differentiation in developing pancreas. *Dev Biol*. 2010;347(1):216-27. Epub 2010/09/03. doi: S0012-1606(10)01035-3 [pii] 10.1016/j.ydbio.2010.08.024. PubMed PMID: 20807526.
57. Gjerdrum C, Tiron C, Hoiby T, Stefansson I, Haugen H, Sandal T, et al. Axl is an essential epithelial-to-mesenchymal transition-induced regulator of breast cancer metastasis and patient survival. *Proc Natl Acad Sci U S A*. 2010;107(3):1124-9. Epub 2010/01/19. doi: 0909333107 [pii] 10.1073/pnas.0909333107. PubMed PMID: 20080645; PubMed Central PMCID: PMC2824310.
58. Koorstra JB, Karikari CA, Feldmann G, Bisht S, Rojas PL, Offerhaus GJ, et al. The Axl receptor tyrosine kinase confers an adverse prognostic influence in pancreatic cancer and represents a new therapeutic target. *Cancer Biol Ther*. 2009;8(7):618-26. Epub 2009/03/03. doi: 7923 [pii]. PubMed PMID: 19252414; PubMed Central PMCID: PMC2678175.
59. Lemke G, Rothlin CV. Immunobiology of the TAM receptors. *Nat Rev Immunol*. 2008;8(5):327-36. Epub 2008/04/19. doi: nri2303 [pii] 10.1038/nri2303. PubMed PMID: 18421305; PubMed Central PMCID: PMC2856445.
60. Cosemans JM, Van Kruchten R, Olieslagers S, Schurgers LJ, Verheyen FK, Munnix IC, et al. Potentiating role of Gas6 and Tyro3, Axl and Mer (TAM) receptors in human and murine platelet activation and thrombus stabilization. *J Thromb Haemost*. 2010;8(8):1797-808. Epub 2010/06/16. doi: 10.1111/j.1538-7836.2010.03935.x JTH3935 [pii]. PubMed PMID: 20546121.
61. Manfioletti G, Brancolini C, Avanzi G, Schneider C. The protein encoded by a growth arrest-specific gene (gas6) is a new member of the vitamin K-dependent proteins related to protein S, a negative coregulator in the blood coagulation cascade. *Mol Cell Biol*. 1993;13(8):4976-85. Epub 1993/08/01. PubMed PMID: 8336730; PubMed Central PMCID: PMC360142.
62. Mann KG, Lawson JH. The role of the membrane in the expression of the vitamin K-dependent enzymes. *Arch Pathol Lab Med*. 1992;116(12):1330-6. Epub 1992/12/01. PubMed PMID: 1456880.
63. Prasad D, Rothlin CV, Burrola P, Burstyn-Cohen T, Lu Q, Garcia de Frutos P, et al. TAM receptor function in the retinal pigment epithelium. *Mol Cell Neurosci*. 2006;33(1):96-108. Epub 2006/08/12. doi: S1044-7431(06)00131-X [pii] 10.1016/j.mcn.2006.06.011. PubMed PMID: 16901715.
64. Linger RM, Keating AK, Earp HS, Graham DK. TAM receptor tyrosine kinases: biologic

- functions, signaling, and potential therapeutic targeting in human cancer. *Adv Cancer Res.* 2008;100:35-83. Epub 2008/07/16. doi: S0065-230X(08)00002-X [pii] 10.1016/S0065-230X(08)00002-X. PubMed PMID: 18620092.
65. Bergers G, Brekken R, McMahon G, Vu TH, Itoh T, Tamaki K, et al. Matrix metalloproteinase-9 triggers the angiogenic switch during carcinogenesis. *Nat Cell Biol.* 2000;2(10):737-44. Epub 2000/10/12. doi: 10.1038/35036374. PubMed PMID: 11025665; PubMed Central PMCID: PMC2852586.
66. Zheng Y, Zhang L, Lu Q, Wang X, Yu F. NGF-induced Tyro3 and Axl function as survival factors for differentiating PC12 cells. *Biochem Biophys Res Commun.* 2009;378(3):371-5. Epub 2008/11/26. doi: S0006-291X(08)02176-1 [pii] 10.1016/j.bbrc.2008.11.049. PubMed PMID: 19027714.
67. Fisher PW, Brigham-Burke M, Wu SJ, Luo J, Carton J, Staquet K, et al. A novel site contributing to growth-arrest-specific gene 6 binding to its receptors as revealed by a human monoclonal antibody. *Biochem J.* 2005;387(Pt 3):727-35. Epub 2004/12/08. doi: BJ20040859 [pii] 10.1042/BJ20040859. PubMed PMID: 15579134; PubMed Central PMCID: PMC1135003.
68. Sasaki T, Knyazev PG, Clout NJ, Cheburkin Y, Gohring W, Ullrich A, et al. Structural basis for Gas6-Axl signalling. *EMBO J.* 2006;25(1):80-7. Epub 2005/12/20. doi: 7600912 [pii] 10.1038/sj.emboj.7600912. PubMed PMID: 16362042; PubMed Central PMCID: PMC1356355.
69. Verstuyf A, Carmeliet G, Bouillon R, Mathieu C. Vitamin D: a pleiotropic hormone. *Kidney Int.* 2010;78(2):140-5. Epub 2010/02/26. doi: ki201017 [pii] 10.1038/ki.2010.17. PubMed PMID: 20182414.
70. Stenhoff J, Dahlback B, Hafizi S. Vitamin K-dependent Gas6 activates ERK kinase and stimulates growth of cardiac fibroblasts. *Biochem Biophys Res Commun.* 2004;319(3):871-8. Epub 2004/06/09. doi: 10.1016/j.bbrc.2004.05.070 S0006291X04010629 [pii]. PubMed PMID: 15184064.
71. Suryanarayan K, Hunger SP, Kohler S, Carroll AJ, Crist W, Link MP, et al. Consistent involvement of the bcr gene by 9;22 breakpoints in pediatric acute leukemias. *Blood.* 1991;77(2):324-30. Epub 1991/01/15. PubMed PMID: 1985699.
72. Neubauer A, Fiebeler A, Graham DK, O'Bryan JP, Schmidt CA, Barckow P, et al. Expression of axl, a transforming receptor tyrosine kinase, in normal and malignant hematopoiesis. *Blood.* 1994;84(6):1931-41. Epub 1994/09/15. PubMed PMID: 7521695.
73. Liu E, Hjelle B, Bishop JM. Transforming genes in chronic myelogenous leukemia. *Proc Natl Acad Sci U S A.* 1988;85(6):1952-6. Epub 1988/03/01. PubMed PMID: 3279421; PubMed Central PMCID: PMC279899.
74. Mahajan NP, Whang YE, Mohler JL, Earp HS. Activated tyrosine kinase Ack1 promotes

prostate tumorigenesis: role of Ack1 in polyubiquitination of tumor suppressor Wwox. *Cancer Res.* 2005;65(22):10514-23. Epub 2005/11/17. doi: 65/22/10514 [pii] 10.1158/0008-5472.CAN-05-1127. PubMed PMID: 16288044.

75. Sainaghi PP, Castello L, Bergamasco L, Galletti M, Bellosta P, Avanzi GC. Gas6 induces proliferation in prostate carcinoma cell lines expressing the Axl receptor. *J Cell Physiol.* 2005;204(1):36-44. Epub 2004/12/18. doi: 10.1002/jcp.20265. PubMed PMID: 15605394.

76. Wu YM, Robinson DR, Kung HJ. Signal pathways in up-regulation of chemokines by tyrosine kinase MER/NYK in prostate cancer cells. *Cancer Res.* 2004;64(20):7311-20. Epub 2004/10/20. doi: 64/20/7311 [pii] 10.1158/0008-5472.CAN-04-0972. PubMed PMID: 15492251.

77. Vajkoczy P, Knyazev P, Kunkel A, Capelle HH, Behrndt S, von Tengg-Kobligk H, et al. Dominant-negative inhibition of the Axl receptor tyrosine kinase suppresses brain tumor cell growth and invasion and prolongs survival. *Proc Natl Acad Sci U S A.* 2006;103(15):5799-804. Epub 2006/04/06. doi: 0510923103 [pii] 10.1073/pnas.0510923103. PubMed PMID: 16585512; PubMed Central PMCID: PMC1458653.

78. Hutterer M, Gunsilius E, Stockhammer G. Molecular therapies for malignant glioma. *Wien Med Wochenschr.* 2006;156(11-12):351-63. Epub 2006/09/01. doi: 10.1007/s10354-006-0308-3. PubMed PMID: 16944367.

79. Hutterer M, Knyazev P, Abate A, Reschke M, Maier H, Stefanova N, et al. Axl and growth arrest-specific gene 6 are frequently overexpressed in human gliomas and predict poor prognosis in patients with glioblastoma multiforme. *Clin Cancer Res.* 2008;14(1):130-8. Epub 2008/01/04. doi: 14/1/130 [pii] 10.1158/1078-0432.CCR-07-0862. PubMed PMID: 18172262.

80. Rochlitz C, Lohri A, Bacchi M, Schmidt M, Nagel S, Fopp M, et al. Axl expression is associated with adverse prognosis and with expression of Bcl-2 and CD34 in de novo acute myeloid leukemia (AML): results from a multicenter trial of the Swiss Group for Clinical Cancer Research (SAKK). *Leukemia.* 1999;13(9):1352-8. Epub 1999/09/14. PubMed PMID: 10482985.

81. Alvarez H, Montgomery EA, Karikari C, Canto M, Dunbar KB, Wang JS, et al. The Axl receptor tyrosine kinase is an adverse prognostic factor and a therapeutic target in esophageal adenocarcinoma. *Cancer Biol Ther.* 2010;10(10). Epub 2010/09/08. doi: 13248 [pii] 10.4161/cbt.10.10.13248. PubMed PMID: 20818175.

82. Gustafsson A, Martuszewska D, Johansson M, Ekman C, Hafizi S, Ljungberg B, et al. Differential expression of Axl and Gas6 in renal cell carcinoma reflecting tumor advancement and survival. *Clin Cancer Res.* 2009;15(14):4742-9. Epub 2009/07/02. doi: 1078-0432.CCR-08-2514 [pii] 10.1158/1078-0432.CCR-08-2514. PubMed PMID: 19567592.

83. Song X, Wang H, Logsdon CD, Rashid A, Fleming JB, Abbruzzese JL, et al. Overexpression

of receptor tyrosine kinase Axl promotes tumor cell invasion and survival in pancreatic ductal adenocarcinoma. *Cancer*. 2010. Epub 2010/10/06. doi: 10.1002/cncr.25483. PubMed PMID: 20922806.

84. Demarchi F, Verardo R, Varnum B, Brancolini C, Schneider C. Gas6 anti-apoptotic signaling requires NF-kappa B activation. *J Biol Chem*. 2001;276(34):31738-44. Epub 2001/06/27. doi: 10.1074/jbc.M104457200 M104457200 [pii]. PubMed PMID: 11425860.

85. Burnier L, Saller F, Kadi L, Brisset AC, Sugamele R, Baudino L, et al. Gas6 deficiency in recipient mice of allogeneic transplantation alleviates hepatic graft-versus-host disease. *Blood*. 2010;115(16):3390-7. Epub 2010/02/09. doi: blood-2009-02-206920 [pii] 10.1182/blood-2009-02-206920. PubMed PMID: 20139094; PubMed Central PMCID: PMC2858482.

86. Fridell YW, Villa J, Jr., Attar EC, Liu ET. GAS6 induces Axl-mediated chemotaxis of vascular smooth muscle cells. *J Biol Chem*. 1998;273(12):7123-6. Epub 1998/04/18. PubMed PMID: 9507025.

87. Goruppi S, Ruaro E, Varnum B, Schneider C. Gas6-mediated survival in NIH3T3 cells activates stress signalling cascade and is independent of Ras. *Oncogene*. 1999;18(29):4224-36. Epub 1999/08/06. doi: 10.1038/sj.onc.1202788. PubMed PMID: 10435635.

88. Shiozawa Y, Pedersen EA, Patel LR, Ziegler AM, Havens AM, Jung Y, et al. GAS6/AXL axis regulates prostate cancer invasion, proliferation, and survival in the bone marrow niche. *Neoplasia*. 2010;12(2):116-27. Epub 2010/02/04. PubMed PMID: 20126470; PubMed Central PMCID: PMC2814350.

89. Shiozawa Y, Pedersen EA, Taichman RS. GAS6/Mer axis regulates the homing and survival of the E2A/PBX1-positive B-cell precursor acute lymphoblastic leukemia in the bone marrow niche. *Exp Hematol*. 2010;38(2):132-40. Epub 2009/11/20. doi: S0301-472X(09)00427-5 [pii] 10.1016/j.exphem.2009.11.002. PubMed PMID: 19922767; PubMed Central PMCID: PMC2815170.

90. Wimmel A, Glitz D, Kraus A, Roeder J, Schuermann M. Axl receptor tyrosine kinase expression in human lung cancer cell lines correlates with cellular adhesion. *Eur J Cancer*. 2001;37(17):2264-74. Epub 2001/10/26. doi: S0959-8049(01)00271-4 [pii]. PubMed PMID: 11677117.

91. Budagian V, Bulanova E, Orinska Z, Duitman E, Brandt K, Ludwig A, et al. Soluble Axl is generated by ADAM10-dependent cleavage and associates with Gas6 in mouse serum. *Mol Cell Biol*. 2005;25(21):9324-39. Epub 2005/10/18. doi: 25/21/9324 [pii] 10.1128/MCB.25.21.9324-9339.2005. PubMed PMID: 16227584; PubMed Central PMCID: PMC1265819.

92. Stitt TN, Conn G, Gore M, Lai C, Bruno J, Radziejewski C, et al. The anticoagulation factor

protein S and its relative, Gas6, are ligands for the Tyro 3/Axl family of receptor tyrosine kinases. *Cell*. 1995;80(4):661-70. Epub 1995/02/24. doi: 0092-8674(95)90520-0 [pii]. PubMed PMID: 7867073.

93. Sun WS, Fujimoto J, Tamaya T. Coexpression of growth arrest-specific gene 6 and receptor tyrosine kinases Axl and Sky in human uterine endometrial cancers. *Ann Oncol*. 2003;14(6):898-906. Epub 2003/06/11. PubMed PMID: 12796028.

94. Chen J, Carey K, Godowski PJ. Identification of Gas6 as a ligand for Mer, a neural cell adhesion molecule related receptor tyrosine kinase implicated in cellular transformation. *Oncogene*. 1997;14(17):2033-9. Epub 1997/05/01. doi: 10.1038/sj.onc.1201039. PubMed PMID: 9160883.

95. Hong CC, Lay JD, Huang JS, Cheng AL, Tang JL, Lin MT, et al. Receptor tyrosine kinase AXL is induced by chemotherapy drugs and overexpression of AXL confers drug resistance in acute myeloid leukemia. *Cancer Lett*. 2008;268(2):314-24. Epub 2008/05/27. doi: S0304-3835(08)00284-X [pii] 10.1016/j.canlet.2008.04.017. PubMed PMID: 18502572.

96. Hasanbasic I, Cuerquis J, Varnum B, Blostein MD. Intracellular signaling pathways involved in Gas6-Axl-mediated survival of endothelial cells. *Am J Physiol Heart Circ Physiol*. 2004;287(3):H1207-13. Epub 2004/05/08. doi: 10.1152/ajpheart.00020.2004 00020.2004 [pii]. PubMed PMID: 15130893.

97. Holland SJ, Powell MJ, Franci C, Chan EW, Frieri AM, Atchison RE, et al. Multiple roles for the receptor tyrosine kinase axl in tumor formation. *Cancer Res*. 2005;65(20):9294-303. Epub 2005/10/19. doi: 65/20/9294 [pii] 10.1158/0008-5472.CAN-05-0993. PubMed PMID: 16230391.

98. Zagzag D, Amirmovin R, Greco MA, Yee H, Holash J, Wiegand SJ, et al. Vascular apoptosis and involution in gliomas precede neovascularization: a novel concept for glioma growth and angiogenesis. *Lab Invest*. 2000;80(6):837-49. Epub 2000/07/06. PubMed PMID: 10879735.

99. Nakano T, Kawamoto K, Higashino K, Arita H. Prevention of growth arrest-induced cell death of vascular smooth muscle cells by a product of growth arrest-specific gene, gas6. *FEBS Lett*. 1996;387(1):78-80. Epub 1996/05/27. doi: 001457939600395X [pii]. PubMed PMID: 8654572.

100. Linger RM, Cohen RA, Cummings CT, Sather S, Migdall-Wilson J, Middleton DH, et al. Mer or Axl receptor tyrosine kinase inhibition promotes apoptosis, blocks growth and enhances chemosensitivity of human non-small cell lung cancer. *Oncogene*. 2013;32(29):3420-31. doi: 10.1038/onc.2012.355. PubMed PMID: 22890323; PubMed Central PMCID: PMC3502700.

FIGURE LEGENDS

Figure 1.1: Structure and analysis of TP-3654. A, TP-3654 compound structure. B, Selectivity analysis of TP-3654. IC₅₀ values are shown for the most potently inhibited kinases. PIM kinase values are K_i values, which were comparable to the IC₅₀ determinations. C, The PIM-1-specific cellular EC₅₀ of TP-3654 was determined in a phospho-BAD (S112) Surefire assay using HEK-293 cells transfected with BAD and PIM-1. The graph represents data from a single experiment, where the EC₅₀ values from four independent experiments (avg = 67 nM) were determined using GraphPad Prism software.

Figure 1.2: Validation of PIM-1 in solid tumor models *in vitro*. A, PIM-1 shRNAs or control shRNA (non-target) were transfected into the UM-UC-3 bladder carcinoma cell line, and PIM-1 mRNA, PIM-1 protein and cell proliferation in a 2D colony formation assay were evaluated. Cells were infected with lentiviral particles overnight, the media was changed and the cells were collected at 48 hrs post-transduction for RNA or protein. A portion of cells were seeded in a 6-well plate at 500 cells/well. Cells were fixed and stained after 10 days of growth. Data for PIM-1 mRNA levels is the average (\pm standard deviation) of 2 independent experiments, while Western blot and colony formation assays are representative of three independent experiments. *p = 0.0028; **p = 0.0002. B, UM-UC-3 (bladder) or C, PC-3 (prostate) cancer cell lines were seeded at 300 or 500 cells/well in a 12-well plate and treated the next day with titrated concentrations of TP-3654 as indicated. Cells were grown for 10 or 6 days respectively, stained for imaging and lysed for quantitation by absorbance at 560 nm. Data are representative of independent experiments evaluating TP-3654 using UM-UC-3 and PC-3 cell lines, with an average EC₅₀ = 1.1 μ M \pm 0.4 μ M (n=4) and 2.2 μ M \pm 0.2 μ M (n=2), respectively.

Figure 1.3: TP-3654 induces apoptosis and inhibits BAD phosphorylation in bladder cancer cell lines. A, The percentage of apoptotic cells was measured using the violet radiometric membrane asymmetry probe/dead cell apoptosis kit for flow cytometry kit from Life Technologies. Cells were seeded in 6-well plates at a concentration of 250,000 cells per well, allowed to grow for 24 hours, and then drug treated with the specified concentrations of TP-3654 or cisplatin (for use as a positive control) for 48 hours. Dyes were added and measured on the flow cytometer and gates were set according to the protocol. The data shown for the TP-0903 treated cells are averages with SEMs compiled from two independent experiments. B, 4 bladder cancer cell lines were tested for basal levels of PIM1, PIM2, and PIM3. Untreated MV4-11 cell lysate was run as a positive control and actin as a loading control. C, UM-UC3 cells were treated with PIM-1 or control siRNA as described in Materials and Methods. Separate, identical blots were treated with antibodies to measure levels of S112 phosphorylated BAD, total BAD, Th37/46 phosphorylated 4EBP1 and total 4EBP1 were measured. D, UM-UC3 Cells were treated for 12 hours with 3, 1, 0.3 and 0.03 μM of TP-3654 and the same proteins analyzed as in C.

Figure 1.4: PIM2 Kinase Expression in Urothelial Carcinoma Cases. A. Immunohistochemical stained sections of Non-invasive low grade papillary urothelial carcinoma (200x) B. Non-invasive high grade urothelial carcinoma (400x) C. Invasive high grade urothelial carcinoma (400x) D. No expression in an invasive high grade urothelial carcinoma (400x)

Figure 1.5: TP-3654 inhibits the growth of established solid tumor xenografts. A, UM-UC-3 bladder carcinoma cells (5×10^6) were implanted per Nu/Nu mouse, with 12 mice/group. Mice were dosed with TP-3654 orally at 200 mg/kg QD, 3 wks, 5 days on 2 days off (red) or with vehicle (black). Caliper measurements (left panel) and tumor weights at the end of the study (middle panel) are shown. No significant change in body weights were observed (right panel). *p

= 0.0028; **p = 0.02. B, PC-3 cells (7.5×10^6) were implanted per male Nu/Nu mouse, with 12 mice/group. Mice were dosed with TP-3654 orally at 200 mg/kg QD, 3 wks, 5 days on 2 days off (red) or with vehicle (black). Caliper measurements (left panel) and tumor weights at the end of the study (middle panel) are shown. No significant change in body weights were observed (right panel). *p = 0.007; **p = 0.0002.

Figure 1.6: Oral PK data for TP-3654. Plasma levels of TP-3654 (ng/mL) in female SD rats were determined using LC/MS. Rats were dosed either by intravenous injection at 2 mg/kg, or orally at 40 mg/kg animal body weight. A simple formulation consisting of 10% polysorbate 20 resulted in the highest exposure (or area under the curve), and showed the highest bioavailability when compared to the IV injected animals.

Figure 2.1: PIM-1 alone interacts with cMYC in AML and MM Cell Lines. A, MV4-11, KASUMI-1 AML cells and ARP-1 MM cells express high levels of PIM-1. MV4-11 cells express PIM-1, 2 and 3. B, IP analysis of the interaction of PIM kinases and cMYC in MV4-11 cells. MV4-11 cells were lysed and the lysates treated with IP-optimized antibodies for PIM-3 (Lane 1), PIM-2 (Lane 2), PIM-1 (Lane 3), and cMYC (Lane 4) as described in materials and methods. Protein-G-agarose beads were used for precipitation. Precipitates were washed 4 times with cold PBS before SDS-PAGE analysis as described in materials and methods. Blots were treated with cMYC antibody for analysis of cMYC expression and possible PIM-cMYC interactions. Separate lysates were treated with beads alone (Lane 6) and beads+AXL (Lane 5) as negative controls. Note that PIM-1 alone (Lane 3) interacts with cMYC as in the positive control (Lane 4). C, KASUMI-1 cells were analyzed as in B. Lane 1-PIM-3, Lane 2-PIM-2, Lane 3-PIM-1, Lane 4-cMYC, Lane 5-AXL, Lane 6-beads alone. D, ARP-1 cells were analyzed as in B. Lane 1-PIM-3, Lane 2-PIM-2, Lane 3-PIM-1, Lane 4-cMYC, Lane 5-AXL, Lane 6-beads alone.

Figure 2.2: PIM-1 siRNA or TP-3654 decreases the PIM-1-cMYC interaction in AML and MM Cell Lines. A, MV4-11 cells were prepared at 1×10^6 cells in 6-well plates and treated with PIM-1 siRNA, using either 6 or 9 μ L of Lipofectamine 2000 transfection reagent as described in materials and methods. Lysates were analyzed for PIM-1 expression to confirm knockdown. IP reactions were carried out in the same manner as described previously, using PIM-1 IP-optimized antibody and protein-G-agarose beads as described in materials and methods. Blots were treated with cMYC primary and mouse secondary antibodies as described in materials and methods. B, ARP-1 cells were prepared at 2×10^6 cells in 6 well plates and immediately treated with 3 μ M (Lane 1), 1 μ M (Lane 2), 300nM (Lane 3), 30nM (Lane 4), 3nM (Lane 5), or vehicle (Lane 6) of TP-3654 for 12 hours prior to lysis, as described in materials and methods. IP reactions were carried out with PIM-1 and cMYC as described in A. C, MV4-11 cells were prepared and drug treated in the same manner as described in B.

Figure 2.3: TP-3654 Induces Apoptosis in AML and MM Cell Lines. MV4-11 or ARP-1 cells were seeded at 2×10^6 cells per well in 6 well plates and immediately treated with the specified concentrations of TP-3654. Cells incubated with the drug for 24 hours prior to lysis. Cells were lysed and Western blots run as described in materials and methods. Blots were assayed for caspase-3 expression to test for apoptotic (cleaved caspase-3) activity in drug treated cells.

Figure 3.1: TP-0903 is a potent AXL kinase inhibitor. Biochemical kinase assays were utilized to determine IC₅₀ values for TP-0903 against the AXL and MERTK kinases. Reactions were run using Invitrogen's TR-FRET LanthaScreen assay and using ATP concentrations at the apparent K_m for each kinase.

Figure 3.2: TP-0903 reduces pAKT levels upon GAS6 stimulation independent of sAXL levels.

A: Pancreatic cancer cell lines (PSN-1 and PL45) were serum starved overnight, treated for 2

hours with TP-0903, and stimulated with Gas6 for 5 minutes. Lysates from these cells were analyzed for total-Akt, phospho-Akt (Ser473) (A), or soluble AXL (B) using the Meso Scale Discovery platform.

Figure 3.3: Cell migration is reduced with AXL inhibitor TP-0903. Images of fixed and crystal violet stained cells after culturing in migration assays in control or drug-treated conditions.

Graph indicates the extent of altered migration versus controls, with P values calculated from data generated from three independent experiments.

Figure 3.4: TP-0903 effectively induces apoptosis in both the PANC-1 and PSN-1 cell lines within 24 hours at concentrations as low as 0.1 μ M. The data shown are percentages of apoptotic cells as measured by flow cytometry gating software, used according to the protocol from Invitrogen. 3 μ M cisplatin was used as a positive control in this experiment, as shown in the 3 μ M group.

Figure 3.5: TP-0903 effectively suppresses expression of EMT marker genes in pancreatic cancer cell lines. The pancreatic cancer cell lines PSN-1 (A, C) and PANC-1 (B, D) were seeded at 1×10^6 cells per well in 6-well plates and allowed to grow for 6 hours before treating with the specified concentrations of TP-0903. For real-time PCR analysis (A, B), RNA isolation was performed 2 hours after drug treatment using the RNeasy kit (QIAGEN) including treatment with DNase to eliminate gDNA contamination. Real-time PCR reactions were carried out using commercially available primers optimized for SYBR-Green (QIAGEN quantitect primer assay) for E-cadherin, snail, and twist and a One-Step SYBR-Green to Ct kit (Invitrogen). The data shown in graphs A and B are averages with corresponding SEMs from two independent experiments. For western blot analysis (C, D), cells were seeded and treated with 1, .3, .1, .03,

and .01 μ M of TP-0903 and cells were lysed (Cell Signaling) 24 hours after drug treatment.

Western blots were carried out as described in materials and methods.

Figure 3.6: Soluble AXL is a potential marker for metastatic cancer progression. A-B: The evaluation of Axl expression at the mRNA (by RT-PCR), protein (by western blot), and sAxl (by ELISA) levels. These results suggest a good correlation between the three ($r^2 = 0.61$ for mRNA to sAxl). C: Serum samples from cancer patients were evaluated for sAxl levels. The results indicate a statistically significant difference between the mean of the control (CTL) group and the PDA (panc) group ($p < 0.05$). Furthermore, there appears to be a subgroup of colon, lung, and PDA patients with particularly high sAxl levels.

Figure 3.7: TP-0903 reduces tumor volume in PSN-1 xenograft studies and displays favorable oral pharmacokinetics. A-B, *In vivo* xenograft studies of PSN-1 pancreatic cancer cells showed a significant reduction in tumor volume ($p < 0.001$) but an insignificant decrease in overall body weight ($p > 0.1$) by Student's t-test. C, Pharmacokinetic studies indicated favorable bioavailability.

TABLES

Table 1.1: Biochemical,^a FLT3^b, and hERG^c potency comparison of TP-3654 and SGI-1776

Compound	PIM1 K _i (nM)	PIM2 K _i (nM)	PIM3 K _i (nM)	FLT3 IC ₅₀ (nM)	hERG IC ₅₀ (μM)	MW
SGI-1776	12	980	20	3	<1	405
TP-3654	5	239	42	279	>30	419

^aK_i determined by Reaction Biology, as described in the materials and methods section. ^bFLT3 IC₅₀ determined by Reaction Biology, as described in the materials and methods section.

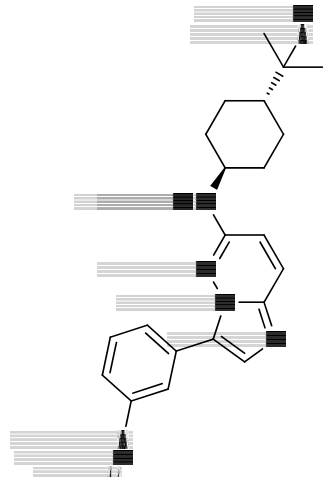
^chERG IC₅₀ determined by WuXi AppTec using the QPatch^{HTX} functional hERG assay described in the materials and methods section.

Table 1.2: PIM kinase expression in urothelial carcinoma

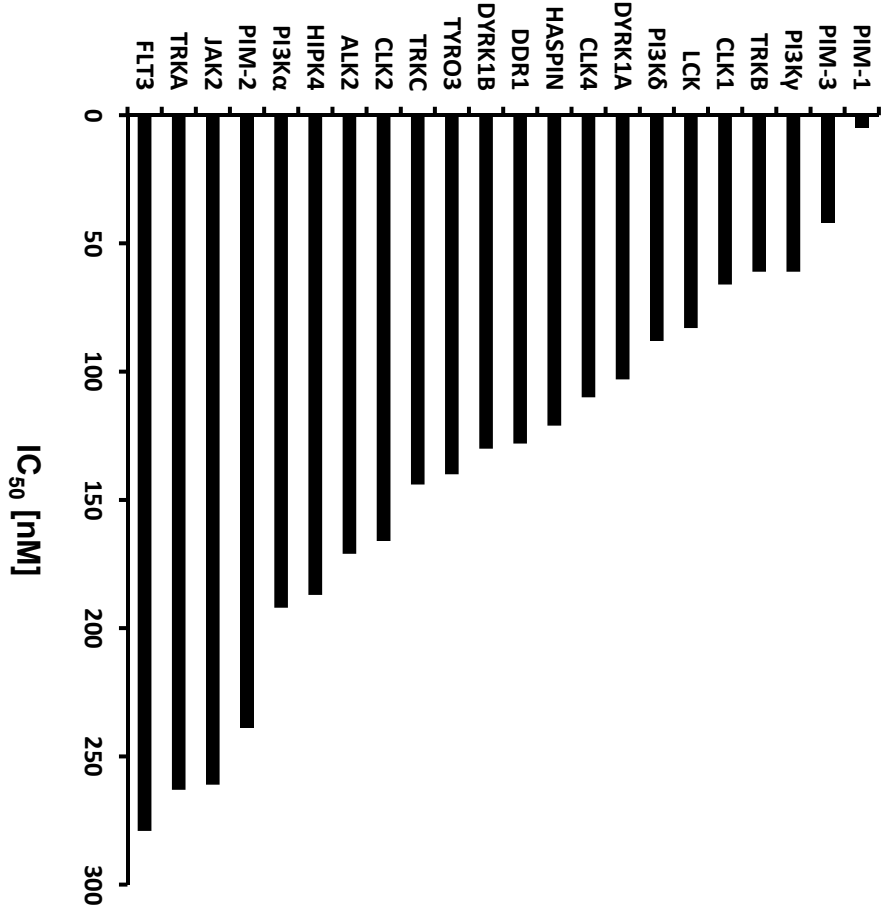
Type	Total N	PIM-1		PIM-2		PIM-3	
		# Positive	%	# Positive	%	# Positive	%
NILG	21	9	43%	7	33%	11	52%
NIHG	32	12	38%	20	63%	9	28%
IHG	84	10	12%	32	38%	11	13%

Number of cases staining positive (score 2-4) or negative (score 0-1) in non-invasive low grade urothelial carcinoma (NILG), non-invasive high grade urothelial carcinoma (NIHG), and invasive high grade urothelial carcinoma (IHG).

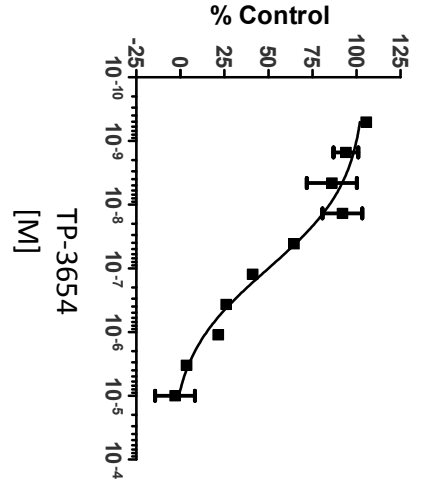
A



B



C



FIGURES

Figure 1.1: Structure and Analysis of TP-3654

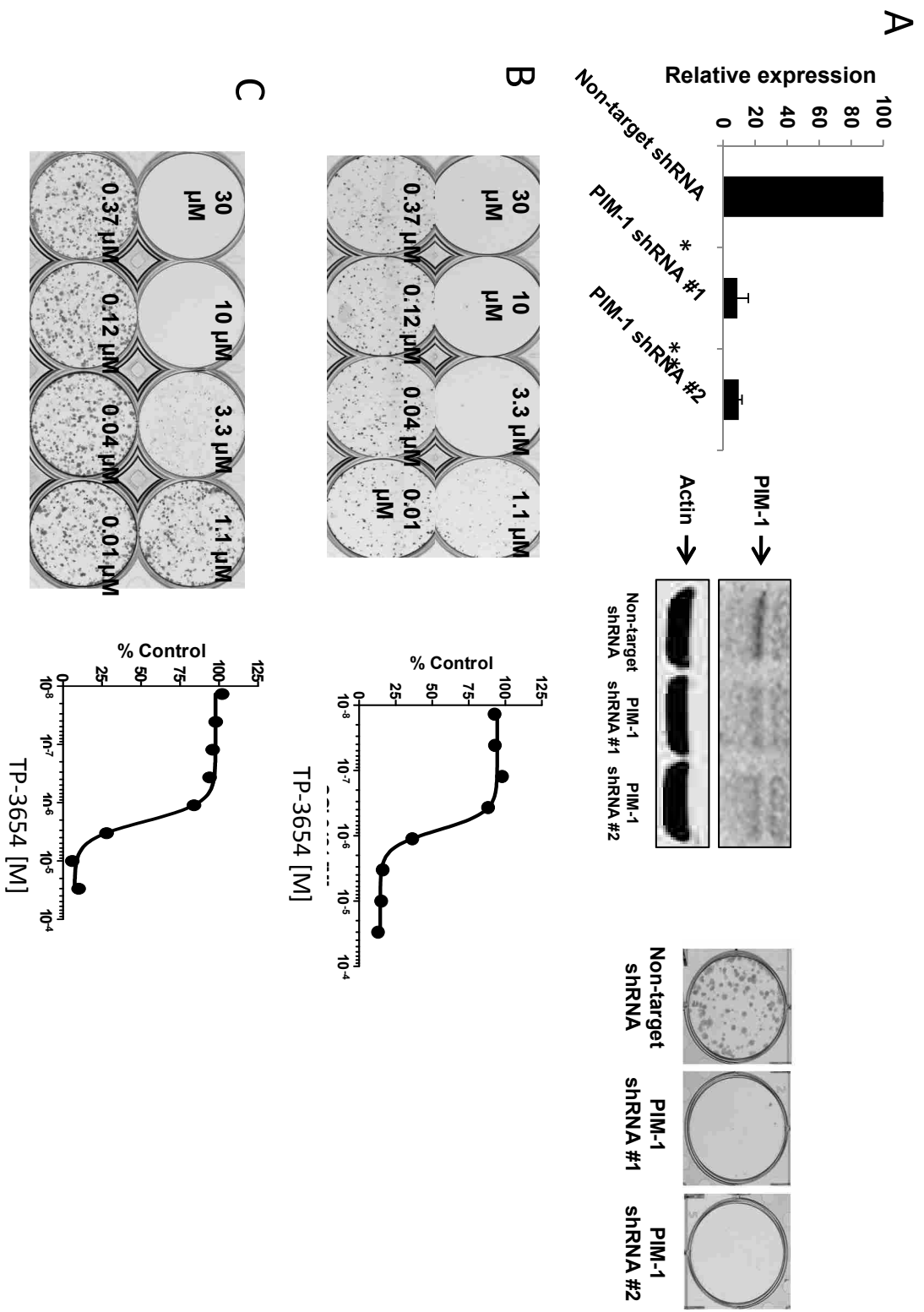


Figure 1.2: Validation of PIM-1 in solid tumor models *in vitro*

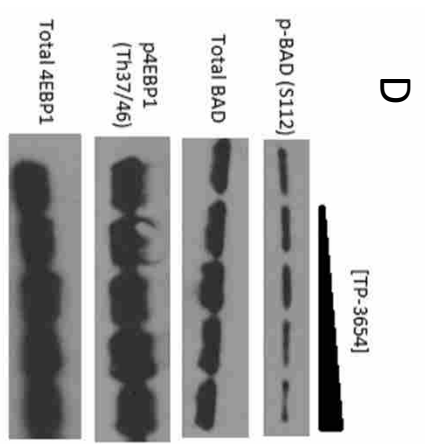
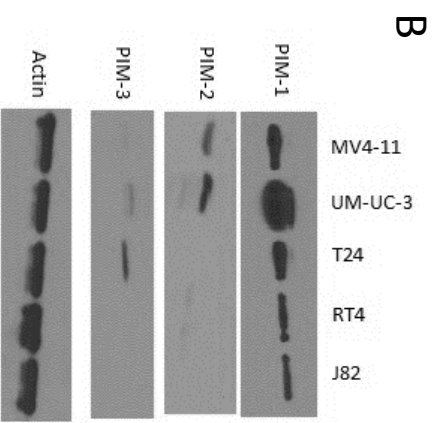
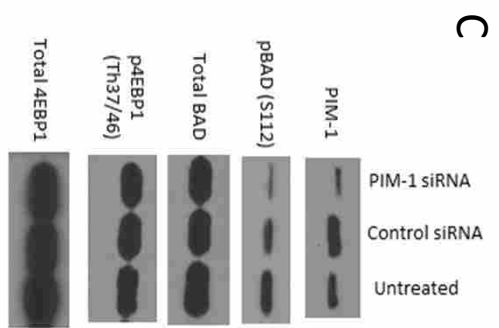
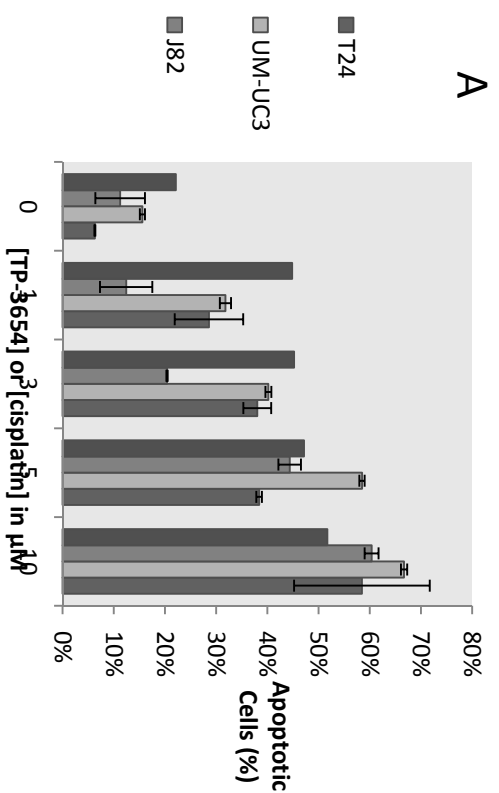


Figure 1.3: TP-3654 induces apoptosis and inhibits BAD phosphorylation in bladder cancer cell lines

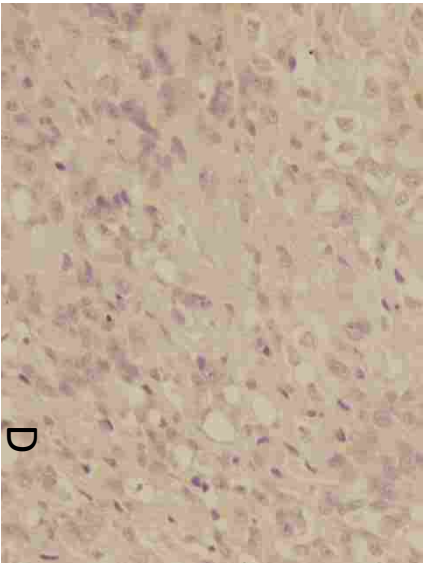
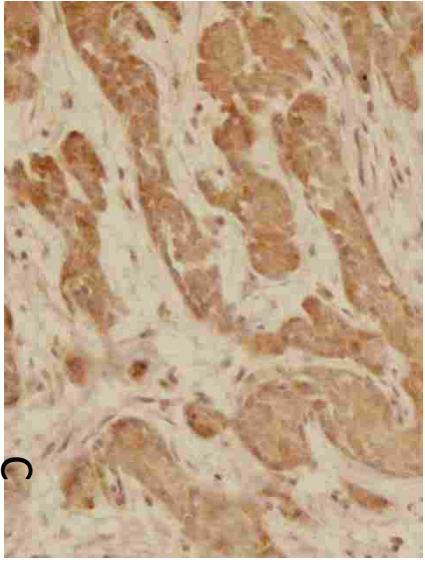
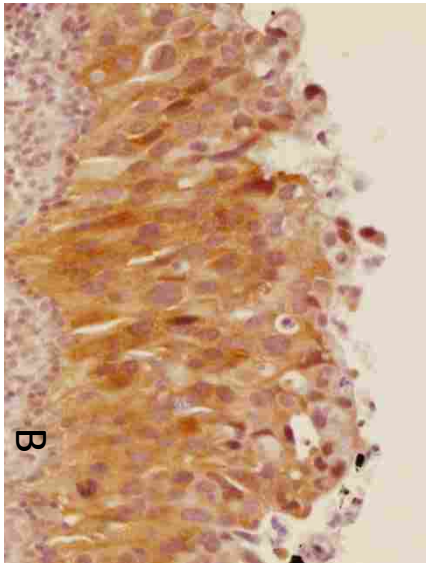
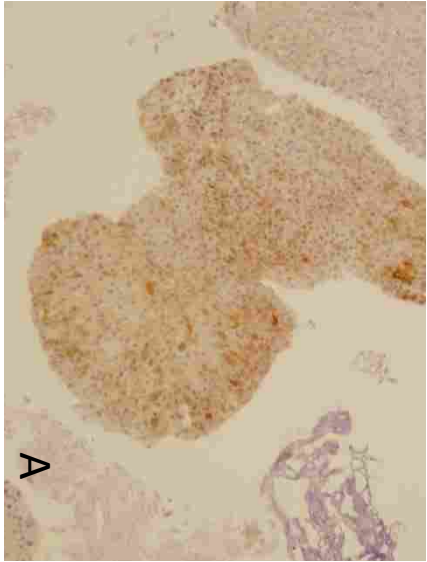


Figure 1.4: PIM-2 Kinase Expression in Urothelial Carcinoma Cases

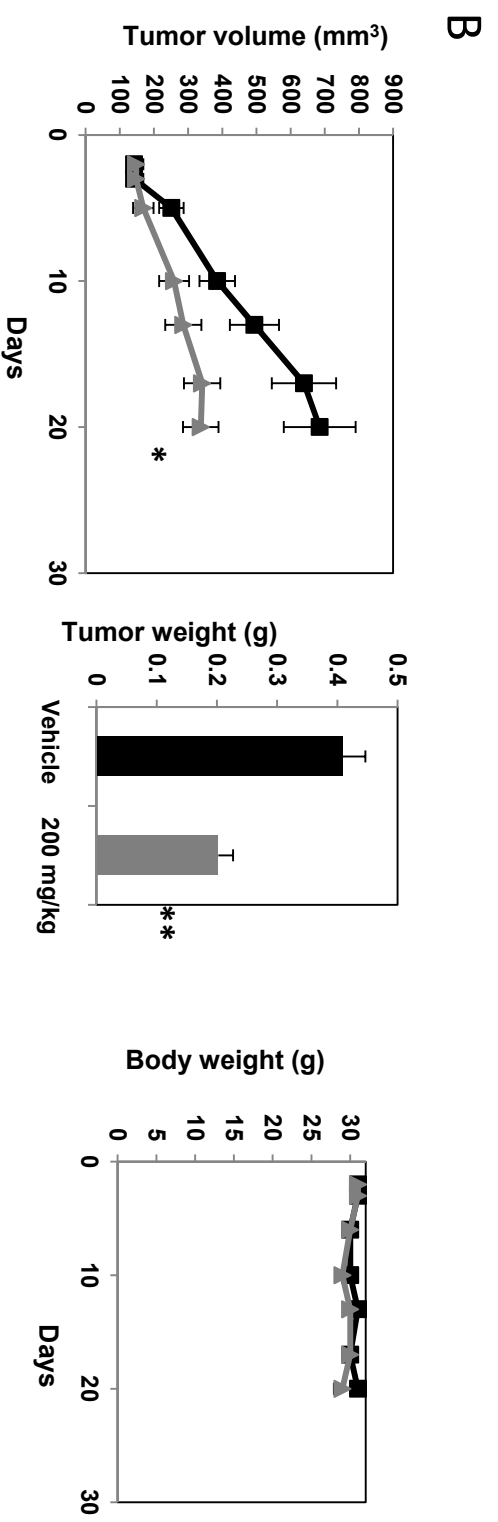
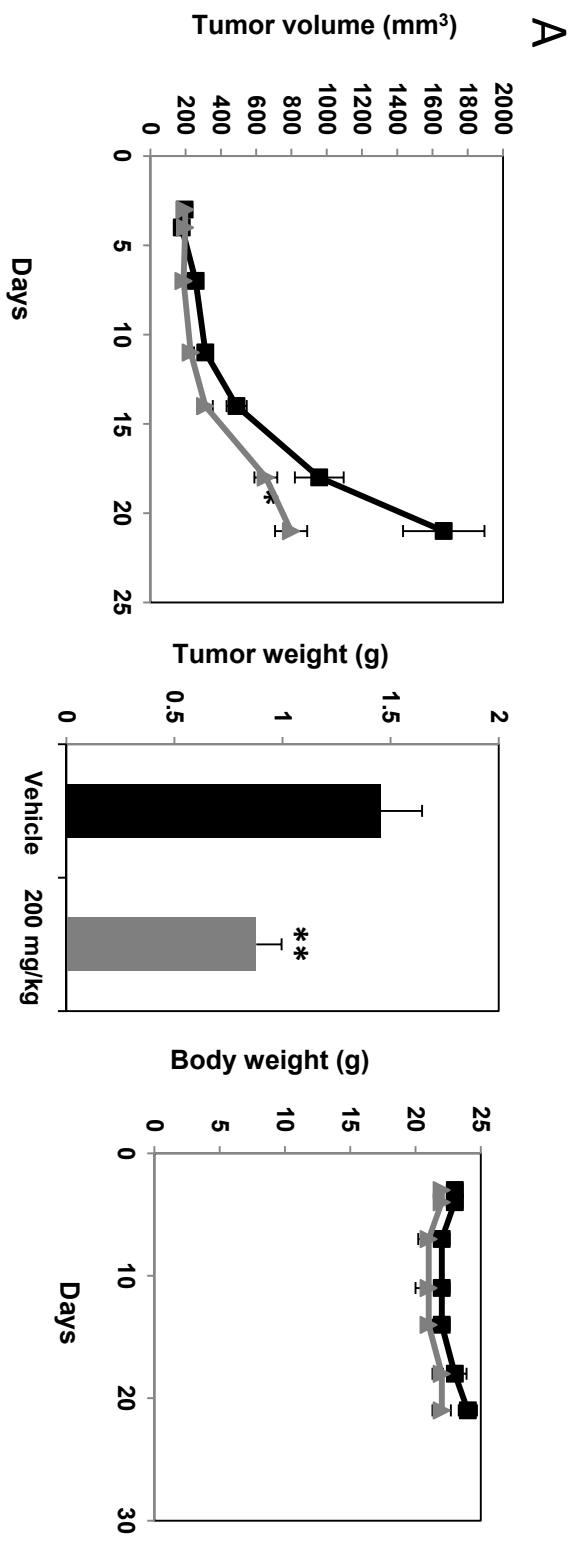


Figure 1.5: TP-3654 inhibits the growth of established solid tumor xenografts

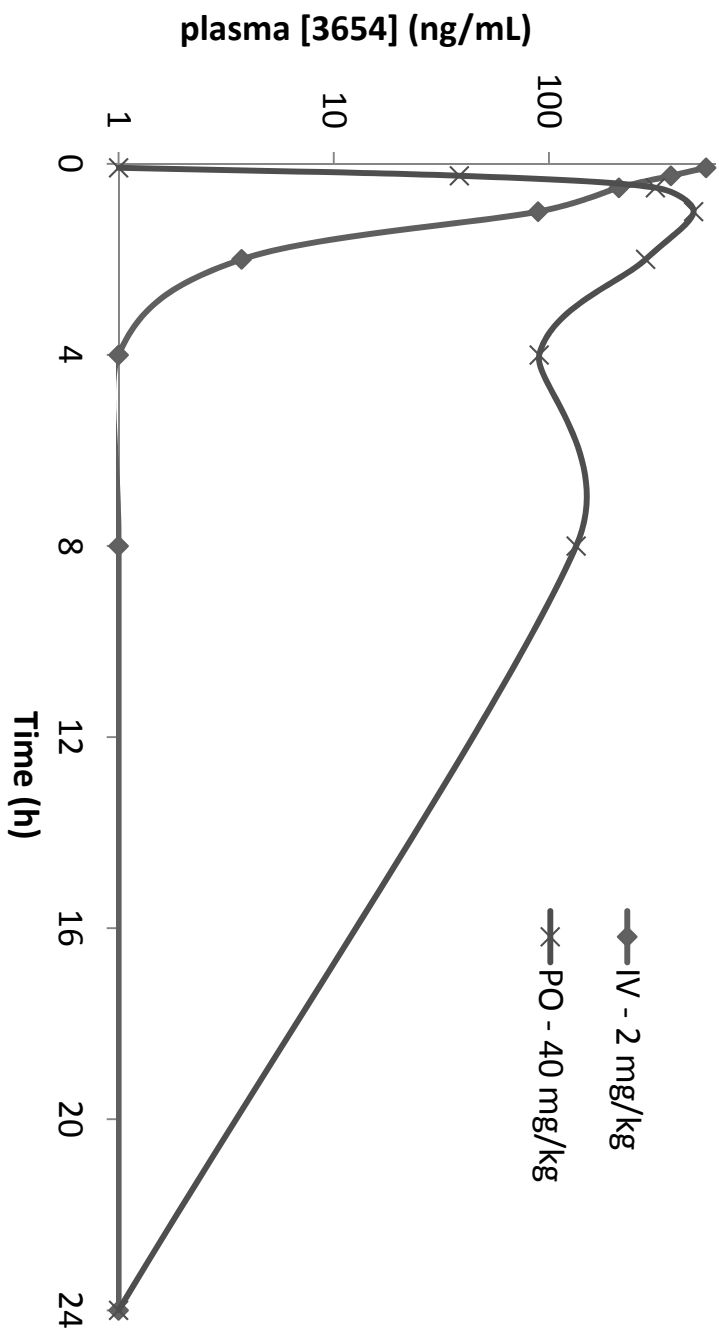


Figure 1.6: Oral PK data for TP-3654

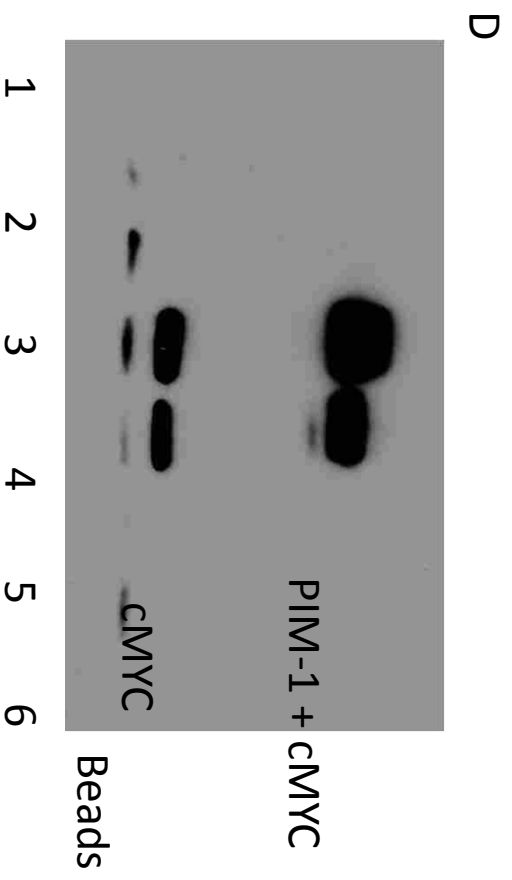
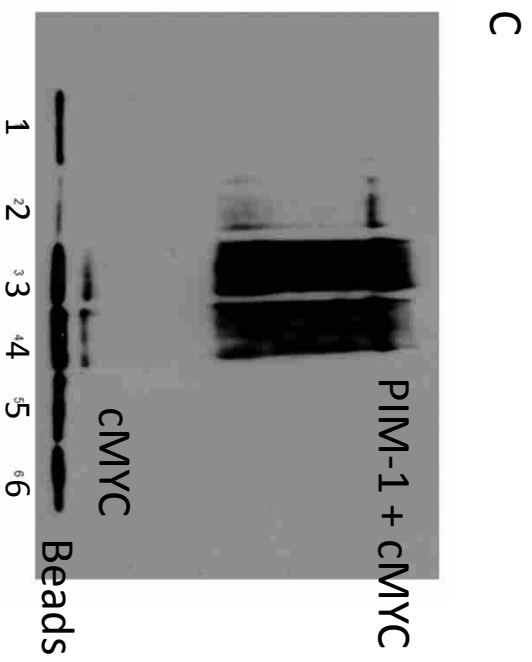
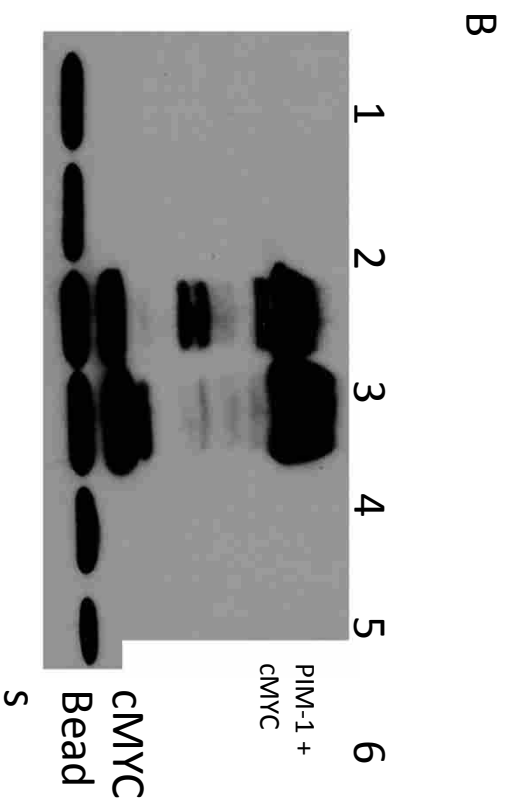
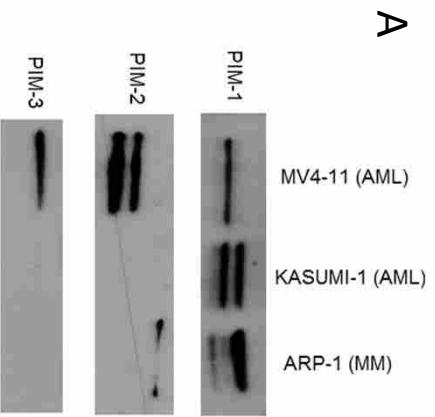


Figure 2.1: PIM-1 alone interacts with cMYC in AML and MM Cell Lines

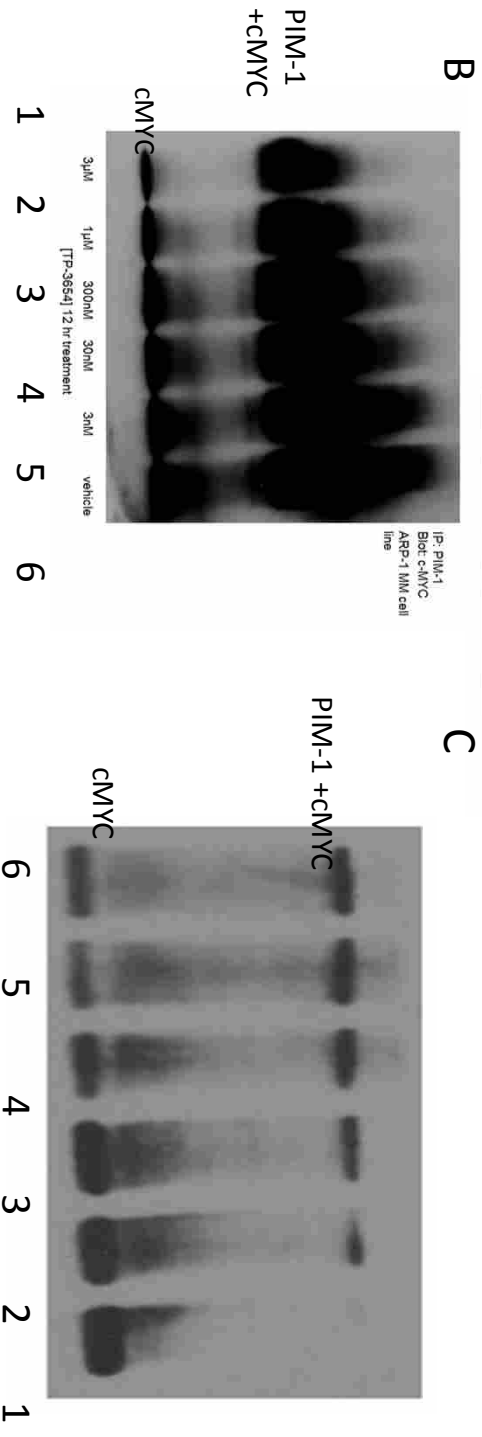
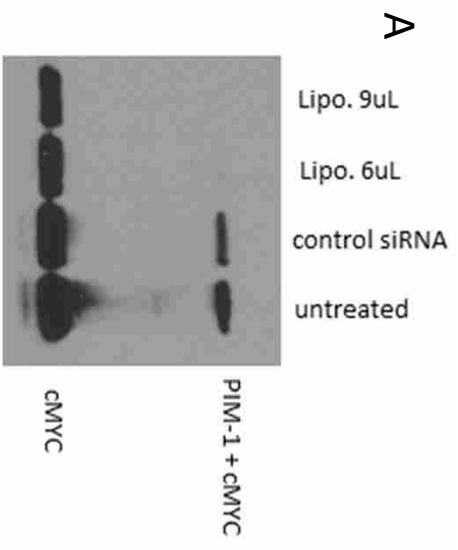


Figure 2.2: PIM-1 siRNA or TP-3654 decreases the PIM-1-cMYC interaction in AML and MM Cell Lines

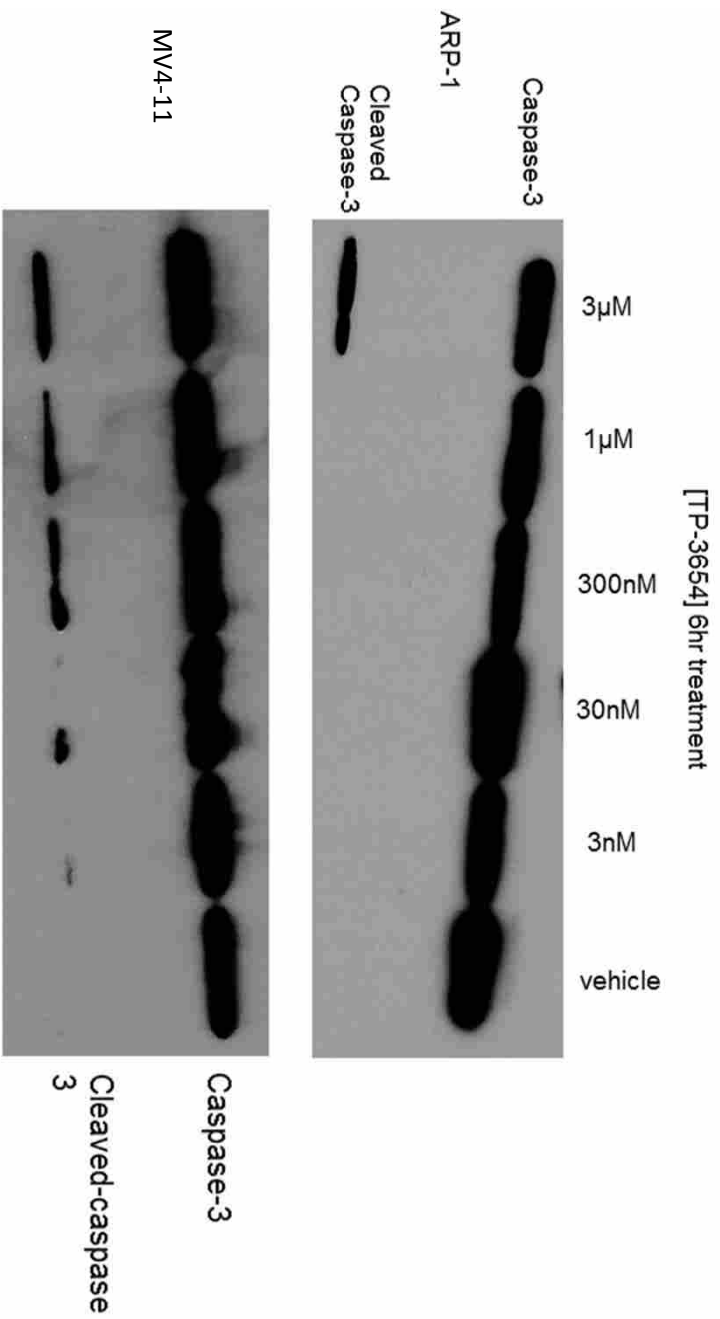


Figure 2.3: TP-3654 Induces Apoptosis in AML and MM Cell Lines

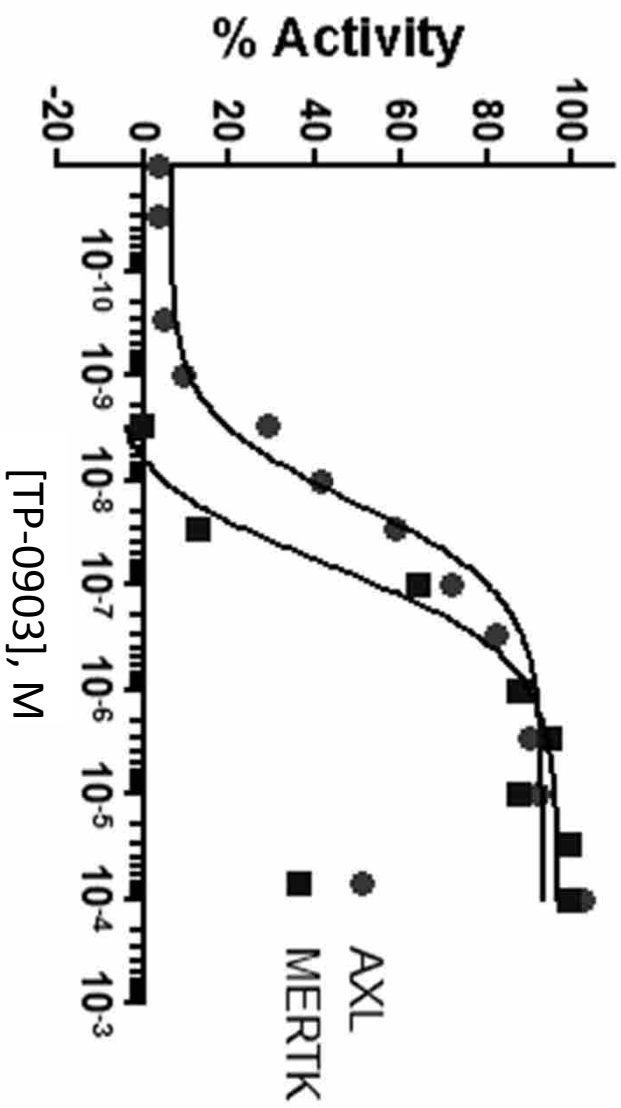
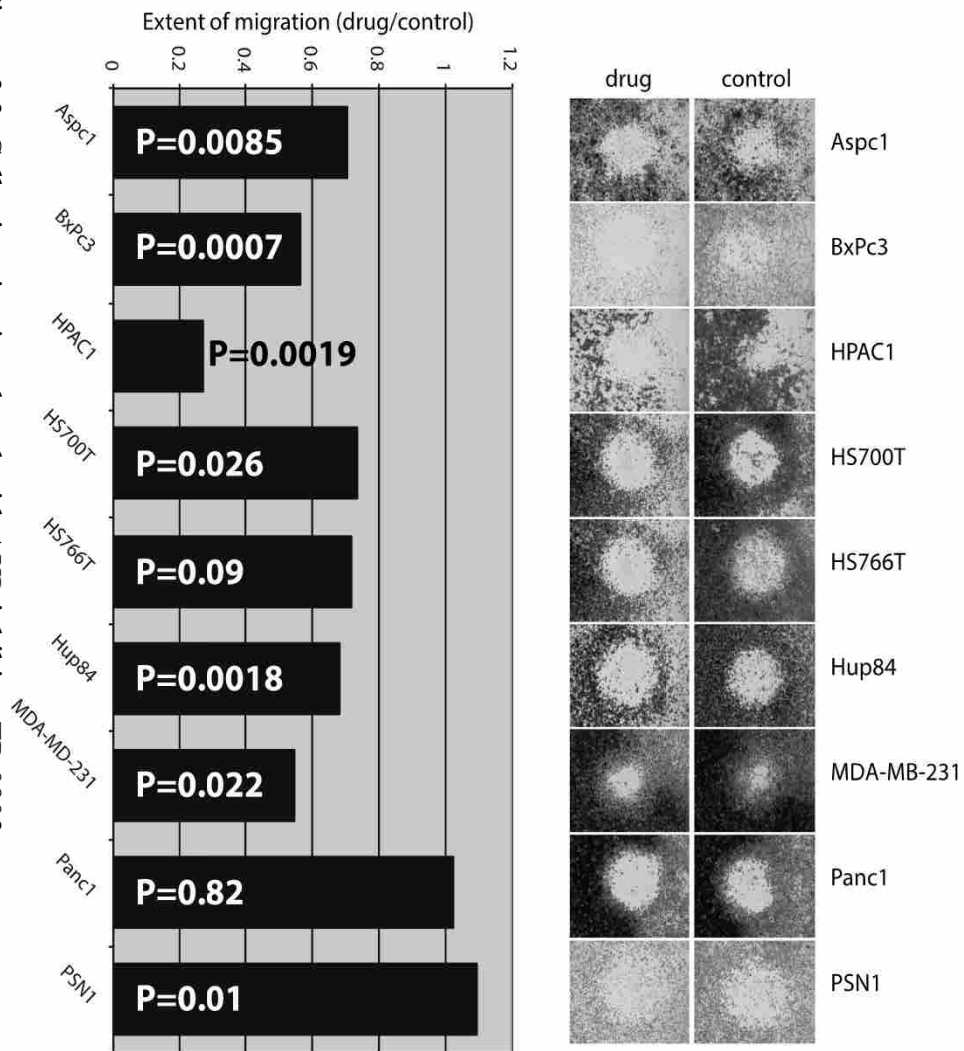


Figure 3.1: TP-0903 is a potent AXL kinase inhibitor

Figure 3.3: Cell migration is reduced with AXL inhibitor TP-0903



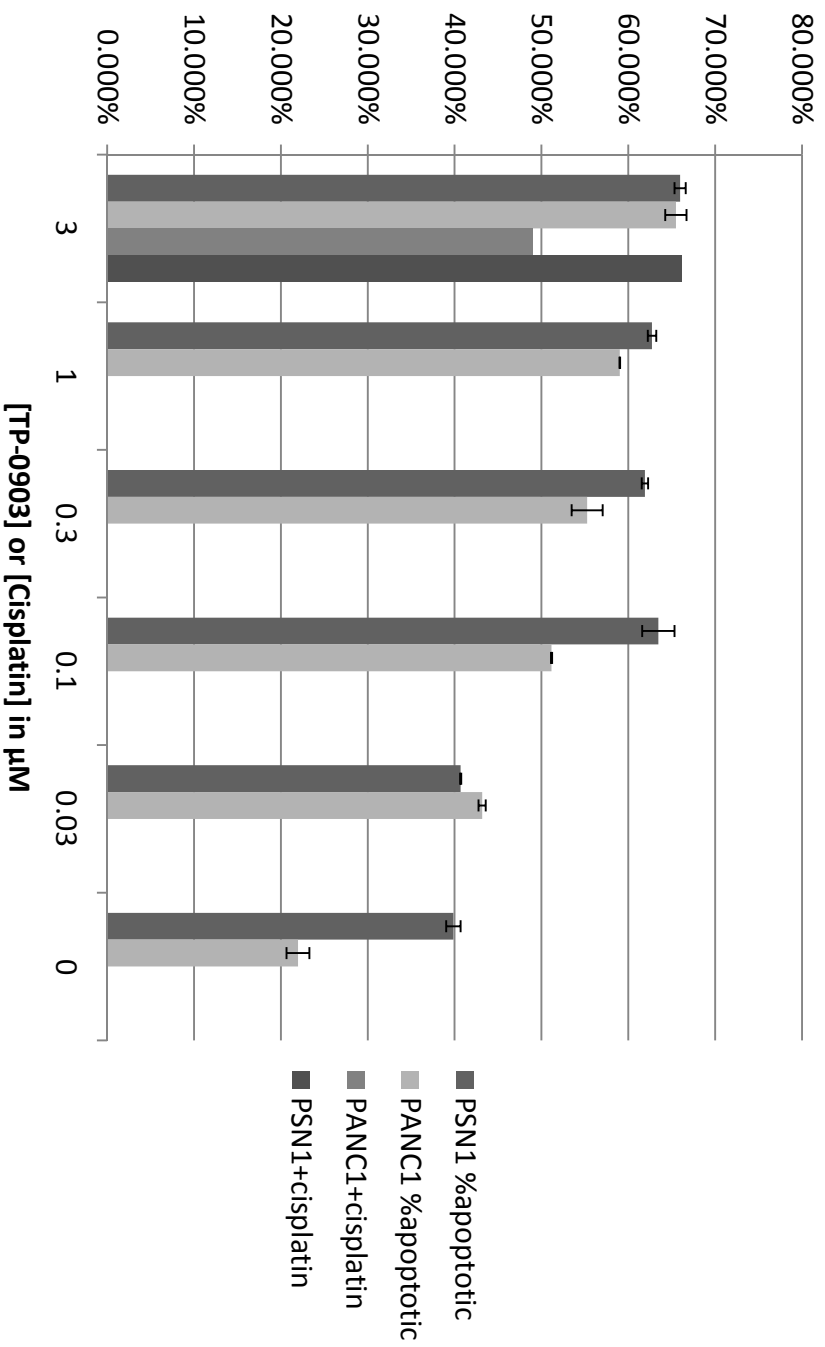


Figure 3.4: TP-0903 effectively induces apoptosis in both the PANC-1 and PSN-1 cell lines within 24 hours at concentrations as low as 0.1 μM

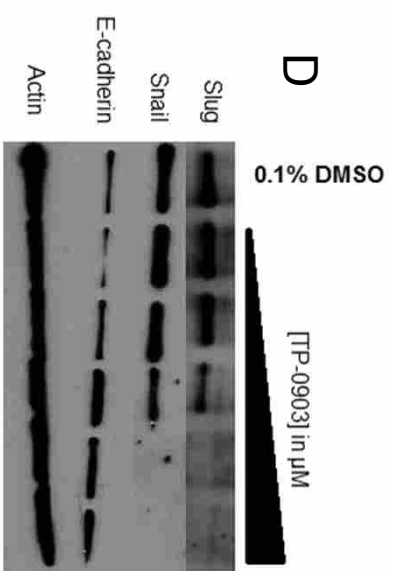
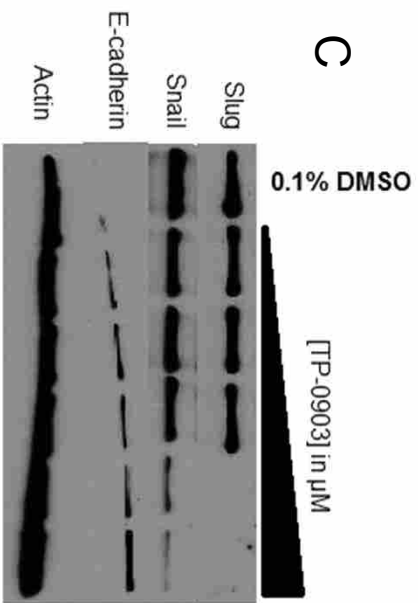
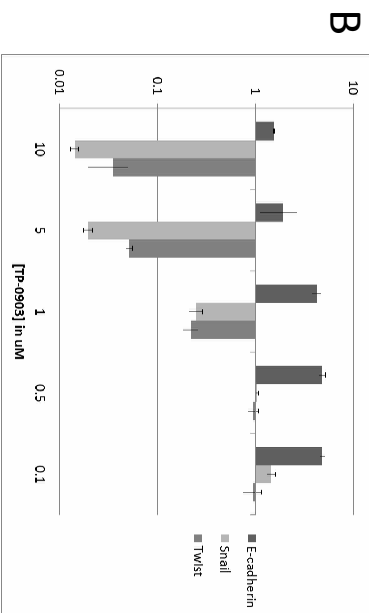
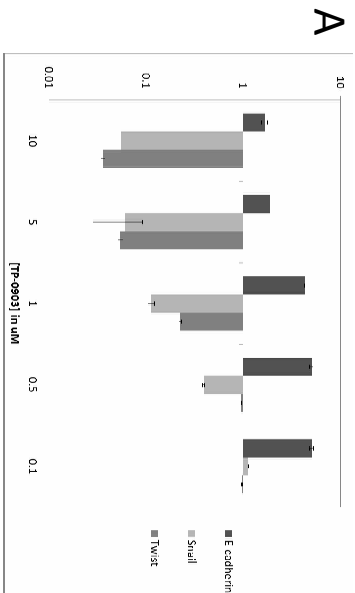


Figure 3.5: TTP-0903 effectively suppresses expression of EMT marker genes in pancreatic cancer cell lines

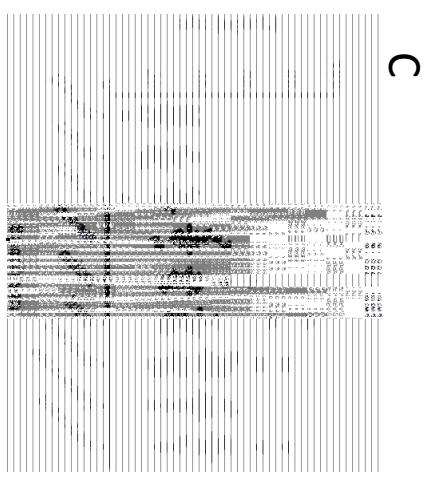
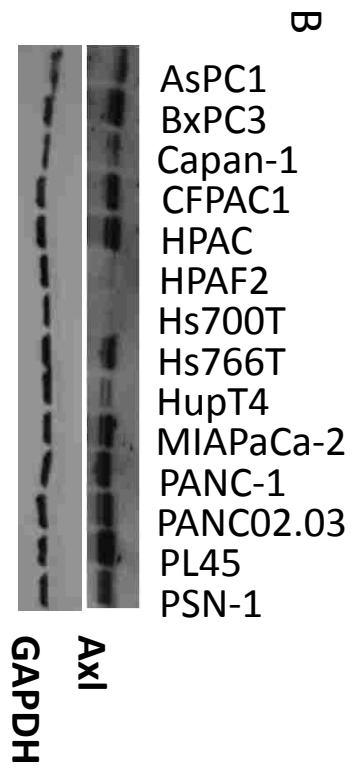
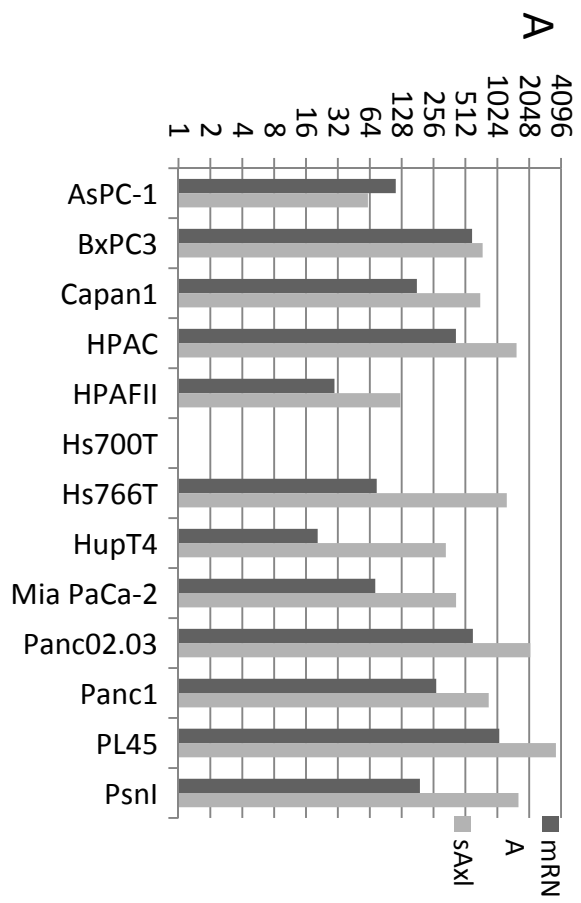


Figure 3.6: Soluble AXL is a potential marker for metastatic cancer progression

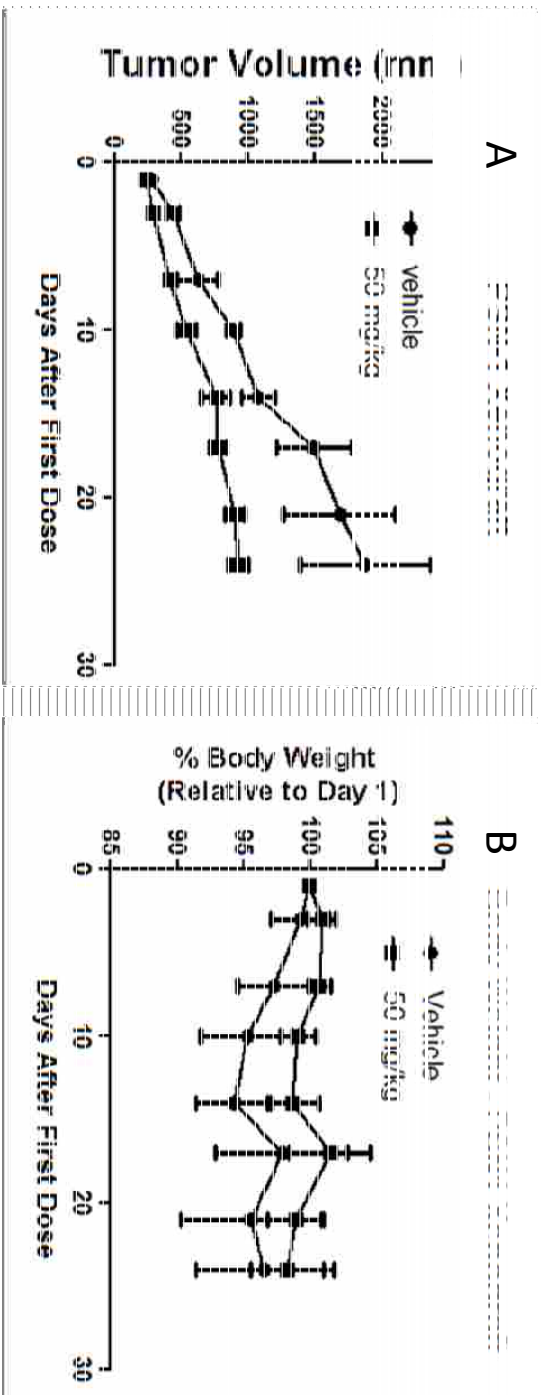


Figure 3.7: TP-0903 reduces tumor volume in PSN-1 xenograft studies and displays favorable oral pharmacokinetics

CURRICULUM VITAE

Kent J Carpenter
718 West Madero Circle
Mesa, AZ 85210
602-510-2681
kent_carpenter@byu.edu

EDUCATION:

2012 B.S. Physiology and Developmental Biology Brigham Young University, Provo, UT.
2014 M.S. (expected) Physiology and Dev Biology Brigham Young University, Provo, UT.

PROFESSIONAL EXPERIENCE:

Dec 2013-present Consultant, Tolero Pharmaceuticals, Lehi, UT. I am currently working as a consultant in drug discovery and development at Tolero Pharmaceuticals Inc. Tolero specializes in the discovery of novel anti-cancer compounds.

2006-2011 Certified Nursing Assistant, Banner Health, Mesa, Arizona. I began working as a hospital CNA in May 2006. I worked seasonally (from June until August) until leaving on my service mission in 2007. I returned in 2008 and worked full time from May 2008 until August of 2009. After that, I continued working in the summers while working on my bachelor's degree. My experience taught me many skills, such as how to communicate effectively and empathetically with patients. My cumulative experience as a CNA totals three years.

RESEARCH TRAINING EXPERIENCE:

2009-2012 Undergraduate research, PDBio Department, Brigham Young University: Research in the lab of Sterling N. Sudweeks, Ph.D. I gained research experience in Dr. Sudweeks's lab working to characterize the channel kinetics of monomeric and heteromeric nicotinic acetylcholine receptors (nAChR's). We characterized how the kinetics of $\alpha 7$ and $\alpha 3\beta 2$ nAChR's were altered with exposure to β -amyloid using electrophysiology in over-expressing *Xenopus* oocytes.

2012-2014 Graduate research, Brigham Young University in the lab of David J. Bearss, Ph.D. I assisted Dr. Bearss in characterizing small molecule inhibitors of growth kinases known to be upregulated in cancer indications. Most notably, I worked to characterize the effect of PIM, AXL, NEK2, PDK1, CDK, and BTK kinase inhibitors in cell culture models of hematological malignancies and solid tumors.

TEACHING EXPERIENCE:

2007-2008 Volunteer English teacher, Deseret International Charities, Ulaanbaatar, Mongolia.

Under Deseret International Charities, I taught English to younger students and adults in Mongolia. I taught English teachers, professional bankers, and a number of college-aged students. Aside from teaching, I performed other services including city cleaning projects, food/clothing delivery, and delivery of medical supplies.

2012-2013 Graduate Teaching Assistant. I have been a teaching assistant as a graduate student for two different professors, including my research adviser, and two different classes. First, I was a teaching assistant for the department's graduate pharmacology class and then for my adviser's cell biology class.

VOLUNTEER EXPERIENCE

2002-2003 Eagle Scout Project. I arranged this scouting project through the City of Mesa Neighborhood Outreach program. The project involved repairing and painting the home of a woman with limited resources. I arranged the entire project, which included replacing the front pergola, repairing the carport roof and, repairing a side gable. Additionally, I arranged a separate two-day event to re-landscape the yards and paint the house with the help of 30 volunteers. My total hours for this project were 41 and the total volunteer hours were 312.

2005-2006 Volunteer, Banner Desert Medical Center, Mesa, AZ. I had the distinct pleasure of serving as a volunteer at Banner Desert Medical Center in Mesa, Arizona. I volunteered an average of 4 hours per week during the school year, and 16 hours per week during the summer (June-August). I assisted nurses and certified nursing assistants in caring for patients in the oncology unit. I would typically replace sharps-containers, bring water to patients, assist with feeding, and make beds. This service experience was especially valuable because it allowed direct contact with patients, and it is what led me to consider a career in medicine. I volunteered a total of 212 hours over this year and was awarded a service learning distinction seal on my diploma.

2007-2008 Volunteer English teacher, Deseret International Charities, Ulaanbaatar, Mongolia. I taught English to younger students and adults in Mongolia, including English teachers, professional bankers, and a number of college- aged students. Preparing and teaching lessons took at least 15 hours per week. Aside from teaching, I helped out in other ways such as city cleaning, and food/clothing delivery. I spent an average of 8 hours per week in these additional service capacities. When not teaching or otherwise serving the communities of Ulaanbaatar, I performed missionary labors for my church, under the direction of Deseret International Charities.

2013 Volunteer, Wasatch Mental Health Intensive Residential Treatment Center, Provo, UT. Last spring, I began volunteering at the Intensive Residential Treatment Center for Wasatch Mental Health. This is a facility where clients transition from a psychiatric hospital environment to prepare to re-enter the community as stable citizens. Volunteering at Wasatch has given me valuable experience in caring for

clients struggling with mental illness. Everything I do as a volunteer involves direct interaction with clients, including helping clients prepare meals, perform daily chores, play games, and other activities.

HONORS AND AWARDS:

11/05	Arizona State University Presidential Scholarship
4/06	Most Outstanding French Student
12/09	Dean's List BYU College of Life Sciences
2/12	PDBio Department Graduate Scholarship
3/13	BYU Cancer Research Center Fellowship Award
5/13	BYU Graduate Student Society Research Presentation Award

MANUSCRIPT PUBLICATIONS:

1. Lingyao Meng, Kent Carpenter, Alexis Mollard, et al. Inhibition of Nek2 by small molecules affects proteasome activity. *Oncotarget*, Feb 2013 (in progress).
2. Kent J Carpenter, Jason M Foulks, Bai Luo, et al. A small molecule inhibitor of PIM kinases as a potential treatment for urothelial carcinomas. *Int J Cancer*, Feb 2014 (in progress).
3. Kent Carpenter, Alexis Mollard, Lee Call et al. Inhibition of the tyrosine kinase receptor AXL blocks cell invasion and promotes apoptosis in pancreatic cancer cells. *Mol Cancer Therapeutics*, Feb 2014 (in progress).
4. Steven L Warner, Kent J Carpenter, and David J Bearss. Metabolic Activators of PKM2. *Future Medicinal Chemistry*, Feb 2014 (in progress).
5. Venkataswamy Sorna, Susie Choi, Lee Call, Jared Bearss, Kent Carpenter, et al. Fragment-Based Design, Synthesis, Biological Evaluation and SAR of 1*H*-benzo[*d*]imidazol-2-yl)-1*H*-indazol Derivatives as Potent PDK1 Inhibitors. *ACS Med Chem Letters*, Feb 2014 (in progress).

PUBLISHED MEETING ABSTRACTS:

1. S Sudweeks, K Carpenter, et al. The effects of B-amyloid on neuronal nicotinic acetylcholine receptors expressed in *Xenopus* oocytes. Society for Neuroscience, New Orleans, LA, 2012.

2. K Carpenter, D Albertson et al. Small molecule inhibitors of PIM kinases as potential treatments for urothelial carcinomas. AACR Washington DC, 2013.
3. K Carpenter, A Ober et al. Inhibition of the tyrosine kinase receptor Axl blocks cell invasion and promotes apoptosis in pancreatic cancer cells. AACR Washington DC, 2013.
4. J Flory, R Brog, K Carpenter et al. Overexpression of Nek2 promotes bortezomib resistance in multiple myeloma cells. AACR Washington DC, 2013.

REFERENCES

David J. Bearss, PH.D.
Founder and Chief Executive Officer
Tolero Pharmaceuticals Inc.
2975 Executive Parkway Suite 320
Lehi, UT 84043
Phone 801-285-6118
Email dbearss@toleropharma.com

Marc D. Hansen, PH.D.
Associate Professor
Physiology and Developmental Biology
Brigham Young University
523 WIDB
Provo, UT 84602
Phone 801-664-7241
Email marchansen@byu.edu

Sterling N. Sudweeks, PH.D.
Graduate Coordinator, Associate Professor
Physiology and Developmental Biology
Brigham Young University
595 WIDB
Provo, UT 84602
Phone 801-422-8752
Email sterling_sudweeks@byu.edu